Molecular Pharmacology Fast Forward. Published on September 14, 2009 as doi:10.1124/mol.109.057554
This article has not been copyedited and formatted. The final version may differ from this version.

Influence of the stereoisomeric position of the reactive acetate groups of the benzo[*b*]acronycine derivative S23906-1 on its DNA alkylation, helix opening, cytotoxic and anti-tumor activities.

Sabine Depauw, Thomas Gaslonde, Stéphane Léonce, Laurence Kraus-Berthier, William Laine, Gaëlle Lenglet, Angèle Chiaroni, Bruno Pfeiffer, Christian Bailly, Sylvie Michel, François Tillequin, Alain Pierré and Marie-Hélène David-Cordonnier*

INSERM U-837-JPARC, Team 4 « Molecular and cellular Targeting for Cancer Treatment », Institut pour la Recherche sur le Cancer de Lille, Place de Verdun, F-59045 Lille, France and IFR114-IMPRT, Lille, France (S.D., W.L., G.L., C.B., M.-H.D.-C.); Laboratoire de Pharmacognosie, Université Paris Descartes, CNRS UMR8638, Faculté des Sciences Pharmaceutiques et Biologiques, 4 avenue de l'Observatoire, F-75270 Paris cedex 06, France (T.G., S.M., F.T.); Laboratoire de Cristallochimie, Institut de Chimie des Substances Naturelles, CNRS UPR 2301, 1 avenue de la Terrasse, F-91198 Gif-sur-Yvette, France (A.C.); Division Recherche Cancérologie, Institut de Recherches SERVIER, Croissy-sur-Seine 78290, France (S.L., B.P., A.P.); Institut de Recherches Internationales SERVIER, Courbevoie 92415, France (L.K.-B.).

Molecular Pharmacology Fast Forward. Published on September 14, 2009 as DOI: 10.1124/mol.109.057554
This article has not been copyedited and formatted. The final version may differ from this version.

a) Running title: **Stereo-selectivity in local DNA opening by S23906-1**

b) *Corresponding author:

Marie-Hélène DAVID-CORDONNIER

Phone : +33 320 16 92 23

Fax : +33 320 16 92 29

e-mail: marie-helene.david@inserm.fr

c) Statistics:

Text: pages **41**

Tables: 1

Schemes: **2**

Figures: **9 (+ 2 supplementary figures)**

References: **40**

Number of words in the Abstract: **229**

Number of words in the Introduction: **722**

Number of words in the Discussion: **1189**

d) Non-standard abbreviations:

GSH: glutathione

AMV: avian myeloblastosis virus

HP: hairpin

ds: double-strand

ss: single-strand

EMSA: electromobility shift assay

bp: base pair

TBE: Tris-borate-EDTA.

Molecular Pharmacology Fast Forward. Published on September 14, 2009 as DOI: 10.1124/mol.109.057554
This article has not been copyedited and formatted. The final version may differ from this version.

Abstract

S23906-1 is a benzo[*b*]acronycine derivative acting as a DNA-alkylating agent through covalent bonding to the exocyclic amino group of guanines and subsequent local opening of the DNA helix. This compound was selected for phase I clinical trials based on its efficient anti-tumor activity in experimental models and its unique mode of action. S23906-1 is the racemate of *cis*-1,2-diacetoxy-6-methoxy-3,3,14-trimethyl-1,2,3,14-tetrahydro-7*H*-benzo[*b*]pyrano[3,2-*h*]acridin-7-one. Here we evaluated the cytotoxic and anti-tumor activities of the two pure *cis*-enantiomers and investigated the mechanism of action of both *cis* and *trans* racemates and their enantiomers in terms of DNA alkylation potency and locally drug-induced DNA helix opening process. Reaction with glutathione, as a detoxification process, was also studied. The *trans*-compounds, both as racemate or separated enantiomers, were found less potent than the corresponding *cis*-derivatives. Among the *cis*-enantiomers, the most efficient one regarding DNA alkylation bears the acetate on the reactive C1 position in the *R*-configuration, both on purified DNA and genomic DNA extracted from cell cultures. By contrast, the most cytotoxic and tumor-active enantiomer bears the C1-acetate in the *S*-configuration. The differences could not be explained by distinct cellular DNA-alkylation levels or covalent bonding to glutathione. However, we showed that the *S*- and *R*-orientations of the acetate on C1 asymmetric carbon lead to different local opening of the DNA, as visualized using nuclease S1 mapping. These different interactions could lead to modulated DNA-repair, protein/DNA interaction, and apoptosis processes.

Molecular Pharmacology Fast Forward. Published on September 14, 2009 as DOI: 10.1124/mol.109.057554
This article has not been copyedited and formatted. The final version may differ from this version.

Introduction

The stereoisomeric position of functional groups in bioactive molecules is known for more than one hundred years to exert an impact on the reactivity of biologically relevant compounds, including drugs. The presence of an asymmetric center in a drug requires specific studies to assess the potency of each isomers. Several cases can be encountered. (*i*) Both enantiomers display similar activities (qualitative and quantitative) fully justifying the clinical use of a racemate, exemplified by flecainide and fluoxetine (anti-arrhythmic and antidepressant drugs, respectively) (Kroemer et al., 1989 ; Magyar et al., 2003). (*ii*) The enantiomers have similar pharmacological effects but different concentration-response efficiencies, such as *S*-(-)-warfarin three- to five-fold more potent as an anticoagulant agent than the *R*-(+) form (Takahashi and Echizen, 2001). (*iii*) One form is active, whereas the other is inactive, as the anti-epilepsy drug *S*-levetiracetam merely inactive in its *R*-form (Gower et al., 1992). (*iv*) Finally, one form is active whereas the other is toxic, such as ethambutol, whose (+)-isomer exhibits potent anti-tubercular properties, while the corresponding (-)-isomer is responsible for optical toxicity in humans (Blessington, 1997) or thalidomide (Melchert and List, 2007). In the field of anticancer agents, chiral specificity is also well documented. The 20(*S*)-isomer of the topoisomerase I inhibitor camptothecin displays significant activity whereas its 20(*R*)-counterpart is 10- to 100-fold less active (Wani et al., 1987). Similarly, the *R*-isomer of the bis-alkylating agent isofosfamide displays an antitumor activity, whereas the *S*-isomer is responsible for the neurotoxicity of racemic isofosfamide (Williams and Wainer, 1999). Stereoselectivity is associated with DNA mono-alkylating agents such as duocarmycin analogues (Cimino et al., 2006) or benzo[*a*]pyrenes (Buening et al., 1978). Sequence selectivity also depends on the configuration of alkylating agents: the (*2S;3S*) *cis*-isomer of the azinomycin epoxide reacts with guanines at TG sites whereas its enantiomer (*2R;3R*) fails (David-Cordonnier et al., 2006).

Molecular Pharmacology Fast Forward. Published on September 14, 2009 as DOI: 10.1124/mol.109.057554
This article has not been copyedited and formatted. The final version may differ from this version.

Altogether, those results and many others evidence the need for determining the precise mechanism of action of all possible isomers of a potential therapeutic agent. This is the purpose of this study. The benzo[*b*]acronycine derivative S23906-1 was selected for its potent cytotoxicity *in vitro* and anti-tumor activity *in vivo* (Guilbaud et al., 2002). It bears two acetoxyl groups at C1 and C2 positions replacing the epoxide group present in the plant natural product acronycine epoxide, isolated from several *Sarcomelicope* species (Brum-Bousquet et al., 1988). The highly reactive epoxide group reacts with water to give *cis*- and *trans*-diols. In order to obtain compounds with similar reactivity but better chemical stability, the epoxide group was replaced by two acetate groups. Additionally, an aromatic ring was linearly fused onto the acronycine basic skeleton, with the idea that it could increase the DNA targeting of acronycine. Due to the position of the two acetate groups on asymmetric carbons, four enantiomeric compounds with *S*- or *R*-configuration at either C1 or C2 atoms have to be considered. The two diastereoisomeric racemates *cis*- and *trans*-1,2-diacetoxy-6-methoxy-3,3,14-trimethyl-1,2,3,14-tetrahydro-7*H*-benzo[*b*]pyrano[3,2-*h*]acridin-7-one could be prepared by acetylation of the corresponding diols, selectively obtained from benzo[*b*]acronycine by osmic oxidation and permanganate oxidation followed by borohydride reduction, respectively. The racemic *cis*-diacetate was selected for further development under the reference S23906-1 since it was identified in preliminary cellular tests as more potent than its *trans*-counterpart S29983-1 (Scheme 1). At the cellular level, S23906-1 induced an increase of the cyclin E level (Léonce et al., 2001), an irreversible S-phase blockade and apoptosis (Costes et al., 2000; Léonce et al., 2001; Kluza et al., 2002) though the generation of replication-dependent double strand breaks (Léonce et al., 2006). At the molecular level, S23906-1 is a DNA alkylating agent, acting through the removal of the acetate group in position 1 (Scheme 1) leading to a reactive carbocation intermediate able to achieve a nucleophilic attack on DNA. It also reacts with glutathione (GSH), another nucleophile of

Molecular Pharmacology Fast Forward. Published on September 14, 2009 as DOI: 10.1124/mol.109.057554
This article has not been copyedited and formatted. The final version may differ from this version.

biological interest (David-Cordonnier et al., 2002, 2003, 2004a). Several experiments argued for a selective bonding of S23906-1 to the exocyclic NH_2 group of guanines as does the marine natural product (and recently registered anticancer drug) ecteinascidin 743 (ET743, Yondelis®) (Pommier et al., 1996). S23906-1 bonding to DNA induces a local destabilization of the DNA helix (David-Cordonnier et al., 2005). However, the impact of the absolute configuration of the drug at C1 and C2 on DNA bonding and destabilization, but also on the cytotoxic and anti-tumor activities, was not addressed and this is the purpose of the present study.

Molecular Pharmacology Fast Forward. Published on September 14, 2009 as DOI: 10.1124/mol.109.057554
This article has not been copyedited and formatted. The final version may differ from this version.

Materials and Methods

Chemical methods. Mass spectra were recorded with a Waters ZQ 2000 spectrometer using electrospray ionization (ES-MS). UV spectra (λ_{max} in nm) were recorded in spectroscopic grade MeOH on a PHILIPS PU 8730 UV/VIS spectrophotometer. IR spectra (n_{max} in cm^{-1}) were obtained from potassium bromide pellets on a Perkin-Elmer 257 instrument. ^{1}H-NMR (d[ppm], *J*[Hz]) spectra were run at 400 MHz and ^{13}C-NMR spectra at 100 MHz, using a Bruker AVANCE-400 spectrometer. The structures of the novel compounds were insured and the signals unambiguously assigned by 2D NMR techniques: ^{1}H-^{1}H COSY, ^{1}H-^{1}H NOESY, ^{13}C-^{1}H HMQC, and ^{13}C-^{1}H HMBC. These experiments were performed using standard Bruker microprograms. Chromatographic columns were conducted using silica gel 60 Merck (20-45 μm) with an overpressure of 300 mbar. Circular dichroism (CD) spectra were recorded with a Jasco J-810 apparatus between 300 and 400 nm, at room temperature. The samples were prepared in methanol at 10^{-4} g/mL

Chemicals. The syntheses of S23906-1 and S28687-1 have been reported previously (Costes et al., 2000). S23906-1 is a racemate with two acetoxy groups on asymmetric carbons at positions 1 and 2 in the relative *cis* configuration. S28687-1 is the racemic *cis*-diol monoacetate at position 2 (see Scheme 1). The corresponding *trans*-racemates S29983-1 and S29850-1 respectively, were also synthesized (Doan Thi Mai et al., 2003). Each of the racemic diesters S23906-1 and S29983-1 were resolved by HPLC on a ChiralCell O.C. column (Chiral Technologies, Strasbourg, France) to give the two corresponding enantiomers. Bromination of S-27589-1, the (+)-enantiomer of S23906-1 gave the corresponding 5-bromo and 5,13-dibromo derivatives. This latter gave suitable crystals permitting X-ray diffraction analysis and establishment of the absolute configuration as (1*S*,2*S*). The absolute

Molecular Pharmacology Fast Forward. Published on September 14, 2009 as DOI: 10.1124/mol.109.057554
This article has not been copyedited and formatted. The final version may differ from this version.

configuration of *trans*-derivatives was determined further on from CD analysis, in comparison with the *cis*-isomers (see Figure 1).

Bromination of (+)*cis*-1,2-diacetoxy-6-methoxy-3,3,14-trimethyl-1,2,3,14-tetrahydro-7*H*-benzo[*b*]pyrano[3,2-*h*]acridin-7-one (scheme 2). *N*-bromosuccinimide (82 mg ; 0.46 mmol) and 2,2'-azobis(2-methylpropionitrile) (1 mg) were added to a solution of (+)*cis*-1,2-diacetoxy-6-methoxy-3,3,14-trimethyl-1,2,3,14-tetrahydro-7*H*-benzo[*b*]pyrano[3,2-*h*]acridin-7-one (150 mg ; 0.307 mmol) in carbon tetrachloride (14 ml). The resulting mixture was stirred 24 h in darkness. After filtration, the solvent was evaporated under reduced pressure. The solid residue was extracted with CH_2Cl_2 (3x50ml). The organic layers were dried over anhydrous $MgSO_4$, filtered and evaporated under reduced pressure. Column chromatography over silica gel (eluent CH_2Cl_2 then CH_2Cl_2/MeOH mixtures of increasing polarity) gave successively (+)*cis*-1,2-diacetoxy-5,13-dibromo-6-methoxy-3,3,14-trimethyl-1,2,3,14-tetrahydro-7*H*-benzo[*b*]pyrano[3,2-*h*]acridin-7-one (101.6 mg ; 51%) and (+)*cis*-1,2-diacetoxy-5-bromo-6-methoxy-3,3,14-trimethyl-1,2,3,14-tetrahydro-7*H*-benzo[*b*]pyrano[3,2-*h*]acridin-7-one (75.4 mg ; 43%). The dibrominated product was crystallized in benzene to give yellow plates, which were analyzed by X-ray diffraction.

(+)*cis*-1,2-diacetoxy-5,13-dibromo-6-methoxy-3,3,14-trimethyl-1,2,3,14-tetrahydro-7*H*-benzo[*b*]pyrano[3,2-*h*]acridin-7-one (scheme 2, compound *a*). Yellow plates, hexagonal-shaped. $[\alpha]^{20}_D$ ($CHCl_3$) = +57°. U.V. : λ nm in MeOH (log ε) : 208 (4.52) ; 241 (4.32) ; 289 (4.57) ; 323 (4.10) ; 414 (3.52). I.R. : 3060 ; 2978 ; 2935 ; 2850 ; 1747 ; 1654 ; 1592 ; 1567 ; 1456 ; 1401 ; 1234 ; 1153 ; 1083 ; 916 ; 730. MS (ES+) : 646, 648 and 650 $[M+H]^+$; 668, 670 and 672 $[M+Na]^+$; 684, 686 and 688 $[M+K]^+$. RMN ^1H ($CDCl_3$) : 1.52 (s, 3H, C3MeB) ; 1.56 (s, 3H, C3MeA) ; 2.11 (s, 3H, COMe1) ; 2.12 (s, 3H, COMe2) ; 3.60 (s, 3H, NMe) ; 4.06 (s,

Molecular Pharmacology Fast Forward. Published on September 14, 2009 as DOI: 10.1124/mol.109.057554
This article has not been copyedited and formatted. The final version may differ from this version.

3H, OMe) ; 5.46 (d, 1H, *J* = 5 Hz, H2) ; 6.75 (d, 1H, *J* = 5 Hz, H1) ; 7.53 (t, 1H, *J* = 8 Hz, H10) ; 7.70 (t, 1H, *J* = 8 Hz, H11) ; 8.00 (d, 1H, *J* = 8 Hz, H12) ; 8.36 (d, 1H, *J* = 8 Hz, H9) ; 8.75 (s, 1H, H8). RMN ^{13}C ($CDCl_3$) : 20.8 (COMe2) ; 21.7 (COMe1) ; 23.3 (C3MeB) ; 24.8 (C3MeA) ; 48.7 (NMe) ; 61.8 (OMe) ; 63.5 (C1) ; 70.2 (C2) ; 78.1 (C3) ; 105.6 (C5) ; 107.5 (C14b) ; 113.6 (C13) ; 117.3 (C6a) ; 126.3 (C10) ; 126.8 (C9) ; 128.0 (C8) ; 129.2 (C7a) ; 130.2 (C11 and C12) ; 130.6 (C12a) ; 135.1 (C8a) ; 144.5 (C13a) ; 152.7 (C14a) ; 156.8 (C4a) ; 159.3 (C6) ; 170.4 (OCO2) ; 171.2 (OCO1) ; 178.9 (C7). Anal. Calcd. For $C_{28}H_{25}Br_2NO_7$: C 51.95 ; H 3.89 ; N 2.16%. Found: C 51.97 ; H 3.95 ; N 2.12%.

(+)*cis*-1,2-diacetoxy-5-bromo-6-methoxy-3,3,14-trimethyl-1,2,3,14-tetrahydro-7*H*-benzo[*b*]pyrano[3,2-*h*]acridin-7-one (scheme 2, compound *b*). Yellow amorphous solid. $[\alpha]^{20}_D$ ($CHCl_3$) = +92°. U.V. : λ nm in MeOH (log ε) : 207 (4.50) ; 238 (4.34) ; 263 (4.33) ; 295 (4.79) ; 440 (3.62). I.R. : 3056 ; 2978 ; 2928 ; 2850 ; 1751 ; 1650 ; 1619 ; 1596 ; 1557 ; 1401 ; 1374 ; 1234 ; 1219 ; 1149 ; 1021. MS (ES+) : 568 and 570 $[M+H]^+$; 590 and 592 $[M+Na]^+$; 606 and 608 $[M+K]^+$. RMN ^1H ($CDCl_3$) : 1.55 (s, 3H, C3MeB) ; 1.61 (s, 3H, C3MeA) ; 1.96 (s, 3H, COMe1) ; 2.04 (s, 3H, COMe2) ; 3.72 (s, 3H, NMe) ; 4.07 (s, 3H, OMe) ; 5.49 (d, 1H, *J* = 5 Hz, H2) ; 6.63 (d, 1H, *J* = 5 Hz, H1) ; 7.43 (t, 1H, *J* = 8 Hz, H10) ; 7.55 (s, 1H, H13) ; 7.57 (t, 1H, *J* = 8 Hz, H11) ; 7.86 (d, 1H, *J* = 8 Hz, H12) ; 8.00 (d, 1H, *J* = 8 Hz, H9) ; 8.88 (s, 1H, H8). RMN ^{13}C ($CDCl_3$) : 20.8 (COMe2) ; 21.1 (COMe1) ; 23.9 (C3MeA) ; 24.5 (C3MeB) ; 43.2 (NMe) ; 61.7 (OMe) ; 65.7 (C1) ; 69.4 (C2) ; 77.8 (C3) ; 102.8 and 103.2 (C5 and C14b) ; 112.0 (C13) ; 115.3 (C6a) ; 125.0 (C10 and C7a) ; 126.9 (C12) ; 128.5 (C8) ; 128.8 (C11) ; 128.9 (C12a) ; 129.8 (C9) ; 136.2 (C8a) ; 142.3 (C13a) ; 148.7 (C14a) ; 156.6 (C4a) ; 159.8 (C6) ; 170.6 (OCO2) ; 170.9 (OCO1) ; 177.4 (C7). Anal. Calcd. For $C_{28}H_{26}BrNO_7$: C 59.16 ; H 4.61 ; N 2.46%. Found: C 59.18 ; H 4.66 ; N 2.43%.

Molecular Pharmacology Fast Forward. Published on September 14, 2009 as DOI: 10.1124/mol.109.057554
This article has not been copyedited and formatted. The final version may differ from this version.

Crystallography. A yellow little plate, hexagonal-shaped, of dimensions (0.25 x 0.25 x 0.10) mm, crystallized from benzene, was chosen for the data collection. The molecular formula was confirmed as $C_{28}H_{25}NO_7Br_2$ giving M_w = 647.31. The compound crystallizes in the space group $P\ 2_12_12_1$ of the orthorhombic system, with four identical molecules in the unit-cell of parameters: a = 9.493(4), b = 13.760(6), c = 20.889(8) Å, V = 2729 Å^3; d_{cal} = 1.576 gcm^{-3}, $F(000)$ = 1304, λ (Mo Kα) = 0.71073 Å, μ =3.018 mm^{-1} were deduced.

Data were measured with a Nonius Kappa-CCD area-detector diffractometer, using a graphite monochromated Mo Kα radiation, in phi and omega scans, up to θ = 27.50°. A full sphere of 43155 data was measured leading to 6242 independent orthorhombic reflections (Rint = 0.052) of which 4926 were considered as observed, having I ≥ 2σ(I). The structure was solved by the Patterson method with program *SHELXS86* (Sheldrick, 1990) and refined by full-matrix least-squares, based upon all the unique F^2 with program *SHELXL97* (Sheldrick, 1997). All hydrogen atoms could be located on Fourier difference maps, but they were fitted at theoretical positions (dC-H = 0.93 to 0.98 Å) and treated as riding, assigned of an isotropic displacement parameter equivalent to 1.12 the one of the bonded atom (1.15 for the H-methyls). The absolute configuration was calculated by the Bijvoët method, from the differences observed between the *Fo* on the one hand, and the *Fcal* on the other hand, on the Friedel pairs (hkl and -h-k -l), due to the anomalous diffusion of the Br atoms, result confirmed by the zero value of Flack factor (-0.010). Thus, refinement of all atomic coordinates and temperature factors of non-hydrogen atoms (349 parameters) converged to $R1(Fo)$ = 0.0371 calculated with the 4926 observed reflections and $wR2(F^2)$ = 0.0777 considering all the 6242 unique data, with a goodness-of-fit S factor of 1.057 [these values became $R1(Fo)$ = 0.0656 and $wR2(F^2)$ = 0.1470 in the inverse configuration]. The residual density was found between -0.71 and 0.75 eÅ^{-3}, near the Br2 atom, the second residue being

Molecular Pharmacology Fast Forward. Published on September 14, 2009 as DOI: 10.1124/mol.109.057554
This article has not been copyedited and formatted. The final version may differ from this version.

of 0.21 eÅ^{-3}. CCDC 661564 file contains the Supplementary Crystallographic data for this paper. These data can be obtained free of charge at //www.ccdc.cam.ac.uk/deposit [or from the Cambridge Crystallographic Data Centre, 12 Union Road, Cambridge CB 1EZ, UK].

Standard proliferation assay. S23906-1 sensitive (KB3-1) or resistant (KB-500) human epidermoid carcinoma cell lines (Léonce et al., 2006) and the human large-cell lung carcinoma NCI-H460 cell line were grown in DMEM medium (Gibco-BRL, France) supplemented with 10 % fetal calf serum, 2 mM *L*-glutamine, 100 units/mL penicillin, 100 µg/mL streptomycin and 10 mM HEPES buffer (pH 7.4). Cytotoxicity was measured by the microculture tetrazolium assay (MTA, Sigma-Aldrich, France) as described (Léonce et al., 1992). Cells were exposed to graded concentrations of drug (nine serial dilutions in triplicate) for 4 doubling times. The IC_{50}, concentration reducing by 50 % the optical density at 540 nm, was calculated by a linear regression performed on the linear zone of the dose-response curve. All the measurements were performed in triplicate.

Cell cycle analysis. L1210 cells (5 x 10^5 cells/mL) were incubated for 21 h with various concentrations of drugs. Cells were then fixed by 70% ethanol (v/v), washed, and incubated in PBS containing 100 µg/mL RNAse and 50 µg/mL propidium iodide for 30 min at 20°C. For each sample, 10^4 cells were analyzed on a XLMCL flow cytometer (Beckman Coulter, France).

Molecular Pharmacology Fast Forward. Published on September 14, 2009 as DOI: 10.1124/mol.109.057554
This article has not been copyedited and formatted. The final version may differ from this version.

Antitumor activity and survival assays. The antitumor activity of the *cis*- racemate and isomers was evaluated on murine colon C38 adenocarcinoma implanted in B6D2F1 (C57B1/6 x DBA2) mice or human NCI-H460 (HTB177) non-small-cell lung carcinoma (American Type Culture Collection, Rockeville, M.D 20852., USA) in nude mice. C38 tumor fragment of approximately 50 mg was sub-cutaneously implanted into the dorsal flank of seven mice. The evaluated compounds were prepared in a mixture of 10% cremophor ELP, 10% ethanol and administrated intravenous at different doses from 1 to 4 mg/kg at days 12 and 22 after tumor graft. Tumor volumes were measured twice a week as a function of length (mm) x width^2 (mm^2)/2. NCI-H460 tumor cells (10^6) were implanted through the chest wall into the left pleural space (i.pl.) of Balb/c nude female mice (Iffa Credo), aged 4 to 6 weeks. Treatment was initiated when the disease was established, 7 days after the injection of NCI-H460 tumor cells, when mediastinal invasion could be observed. Each compound (S23906-1, S27589-1 and S27590-1) was administered by i.v. route, 10 days apart, the first day of treatment being 7 days after the tumor cells injection. Animal mortality was checked daily, and the MST (Median survival time, in days) of each group was calculated. Results were expressed in terms of both the percentage T/C value and number of LTS. Median percentage of T/C = (MST of treated group/MST of control group) x 100, and LTS (long-term survivors) were defined as surviving animals sacrificed at the end of the experiment for which no tumor could be detected by macroscopic examination. The studies have been carried out in accordance with the Declaration of Helsinki.

DNA fragments. The radio-labeled 117-bp and 198 bp DNA fragments were obtained from pBS or pMS1 plasmid digestions (David-Cordonnier et al, 2002) using *Eco*RI and *Pvu*II or *Hind*III and *Xba*I restriction enzymes (BioLabs, France), respectively, in their corresponding

Molecular Pharmacology Fast Forward. Published on September 14, 2009 as DOI: 10.1124/mol.109.057554
This article has not been copyedited and formatted. The final version may differ from this version.

digestion buffers and labeling at the *Eco*RI or *Hind*III sites with α-[^{32}P]-dATP (3000 Ci/mmol, GE Healthcare, France) and AMV reverse transcriptase (Ozyme, France). The double stranded XH-24 oligonucleotide was prepared by labeling one strand using polynucleotide kinase (Invitrogen, France) in the presence of γ-[^{32}P]-ATP (3000 Ci/mmol, GE Healthcare, France) before annealing to the complementary oligonucleotide as previously described (David-Cordonnier et al., 2005). The hairpin oligonucleotide HP-AGA was obtained by heating at 80°C the oligonucleotide followed by a slow decrease of temperature up to 4°C. HP-AGA was then labeled on the 5'-end using PNK as described previously. Both oligonucleotides were ordered from Eurogentec (Belgium). The radio-labeled DNA fragments were removed from the excess of radioactive nucleotide by electrophoresis on a non-denaturing 10 % (w/v) polyacrylamide gel and subsequent excision of the desired portion of the gel containing the radio-labeled products. This gel portion was then crushed and the radio-labeled DNA was eluted overnight against 400 µl of elution buffer (500 mM ammonium acetate, 10 mM magnesium acetate) prior to be filtered and ethanol precipitated.

Gel shift studies. A typical DNA alkylation reaction consisted of incubating 8 µL of radio-labeled DNA with 2 µL of 10X buffer (10 mM Na cacodylate, pH 7.0) and 10 µL of the drug at the desired concentration for the indicated time in the dark at 37°C prior to adding 5 µL loading buffer containing tracking dyes. The DNA samples were resolved by electrophoresis under non-denaturing conditions in 10 % polyacrylamide gels for about 5 h at 300 V at room temperature in TBE buffer (89 mM Tris base, 89 mM boric acid, 2.5 mM Na_2EDTA, pH 8.3). Gels were then transferred to a Whatman 3MM paper, dried under vacuum at 80°C and analyzed on a Molecular Dynamics 445SI phosphorimager (Molecular Dynamics, Sunnyvale, CA). For studying the competition for DNA alkylation using glutathione (GSH), 400 µM of

Molecular Pharmacology Fast Forward. Published on September 14, 2009 as DOI: 10.1124/mol.109.057554
This article has not been copyedited and formatted. The final version may differ from this version.

GSH was incubated for 1 hour with 5, 10, 20 or 50 µM of the compounds of interest. The radio-labeled DNA fragment was then added and the samples were further incubated at 37°C for 2 hours. The reaction was then stopped and the samples subjected to electrophoresis and analyzed as described above.

HPLC and mass spectra analysis. For HPLC-fluorometric analysis, high performance liquid chromatographic analysis were carried out using a Jasco HPLC system equipped with a quaternary pump with on-line autosampler, Jasco UV-975 UV/vis detector (Jasco, France) and RF-551 spectrofluorimetric detector (Shimadzu, Japan). 50 µM of the *cis*-racemate S23906-1 or purified *cis*- enantiomers S27589-1 and S27590-1 were incubated alone or with 50 µM of GSH (Sigma, France) for 24 hours at 37°C in ammonium acetate 1mM, pH 7.15. 50 µl of samples were injected in a modulo-cart QS Uptispher 5-FT column (150 mm × 2 mm, Interchim, France) at flow rate of 0.2 ml/min of mobile phase (18% acetonitrile, 23% methanol, 59% H_2O, formic acid 0.1%, pH 2.9). Fluorimetric spectra were recorded at 510 nm for an excitation wavelength of 354 nm. For HPLC-EI-MS, the HPLC analysis were performed using a Perkin Elmer Series 200 LC pump equipped with an on-line Perkin Elmer series 200 auto-sampler coupled to a simple-quadrupole mass spectrometer API 3000 (Perkin-Elmer, France) equipped with an ion-spray (nebulizer-assisted electrospray) source (Sciex, Toronto, Canada). Full scan ion spray mass spectra were acquired at unit resolution by scanning from m/z 100 to 1500 with a step size of 0.1 Da and a dwell time of 2 ms. Data were acquired and processed by Analyst 1.4.1 workstation. Peaks at the relevant mass/charge (determined in parallel by EI-MS and MS-MS as previously described in David-Cordonnier et al., 2003) were extracted using the Analyst software to identify the various time of elution of the HPLC-separated products.

Molecular Pharmacology Fast Forward. Published on September 14, 2009 as DOI: 10.1124/mol.109.057554
This article has not been copyedited and formatted. The final version may differ from this version.

Detection of DNA adducts in cells. KB3-1 epidermoid carcinoma cells were grown in DMEM-glutaMAX medium (Gibco-BRL, France) supplemented with 10% fetal calf serum (FCS), penicillin (100 IU/ml, Gibco-BRL, France) and streptomycin (100 µg/ml, Gibco-BRL, France) in a humidified atmosphere at 37°C under 5% CO_2. 1.5 x 10^6 KB3-1 cells were grown for 24 h in 100 mm diameter dishes with 5 ml of culture medium, prior to the treatment of the cells using increasing concentrations (1, 2.5, 5, 7.5, 10 and 15 µM) of S23906-1, S27589-1, S27590-1, S29983-1, S70255-1 or S70256-1. After 24 hours, treated cells were collected by centrifugation (1300 rpm, 5 min), washed twice with 10 ml PBS buffer (Gibco-BRL, France) and dissolved in 2 ml of PBS supplemented with 5 mM $MgCl_2$. The cell lysis was initiated by addition of 200 µl of 10 % SDS and mild agitation for 5 min followed by addition of proteinase K (80 µl at 10 mg/ml, Sigma, France) for a further 5 min of mild agitation. Finally, 200 µl of 0.1 M EDTA pH 7.5 were added and the mixture was incubated 4 hours at 37°C. After addition of 80 µl of 5 M NaCl, the genomic DNA was extracted using 3 mL of phenol/chloroform/isoamylic alcohol (25:24:1) and further centrifugation at 4,000 rpm for 10 min, followed by two additional extractions using 3 mL of chloroform/isoamylic alcohol (24:1) mixture. Finally, the genomic DNA was precipitated with cold ethanol and centrifugation at 11,000 rpm for 30 min. The UV absorption of the final solution at 260 nm was used to estimate the quantity of collected DNA. The fluorescence of the benzo-*b*-acronycine core molecule covalently linked to DNA was measured using a SPEX Fluorolog spectrofluorimeter (Ivon Jobin, Longjumeau, France) with an excitation wavelength at 300 nm and an emission range from 450 to 560 nm. The values at the emission peak of 510 nm were used to draw the graph.

Nuclease S1 digestion. The radio-labeled 117-bp DNA fragment were incubated over-night with various di-acetate derivatives at various concentrations at 37°C in 20µL of sodium

Molecular Pharmacology Fast Forward. Published on September 14, 2009 as DOI: 10.1124/mol.109.057554
This article has not been copyedited and formatted. The final version may differ from this version.

cacodylate (1 mM pH 7.0). The digestion was performed by the addition of 4 units of S1 nuclease (Roche, France) in the appropriate nuclease S1 specific buffer for further 15 min incubation. The DNA samples were then mixed with 5 µL of native loading buffer containing tracking dyes subjected to electrophoresis on a 10 % native polyacrylamide gel at 300 V at room temperature in TBE buffer. The gel was then dried and analyzed on the Molecular Dynamics 445SI phosphorimager (GE Healthcare, France).

Molecular Pharmacology Fast Forward. Published on September 14, 2009 as DOI: 10.1124/mol.109.057554
This article has not been copyedited and formatted. The final version may differ from this version.

Results

Structural characterization of the molecules

The racemic diesters S23906-1 and S29983-1 were resolved into the corresponding enantiomers using chiral HPLC. In order to determine the absolute configuration using X-ray diffraction, the S27589-1 (+)-enantiomer of S23906-1 was subjected to bromination with *N*-bromosuccinimide. This reaction led to the corresponding 5-bromo and 5,13-dibromo derivatives which could be easily separated on a preparative scale using column chromatography over silica gel. (+)*cis*-1,2-Diacetoxy-5,13-dibromo-6-methoxy-3,3,14-trimethyl-1,2,3,14-tetrahydro-7*H*-benzo[*b*]pyrano[3,2-*h*]acridin-7-one crystallized from benzene as yellow hexagonal-shaped plates which were submitted to X-ray crystallographic analysis. An *ORTEP* view of the molecule is shown in Figure 1A, with the absolute configuration and the atomic numbering. The analysis of the mean planes and torsion angles values indicates that the five rings are roughly coplanar if are omitted the C3 atom and the nitrogen N14 situated at respectively 0.820(3) and -0.611(3) Å from the mean plan of the other nineteen atoms. More precisely, the molecule can be considered as two planar entities, the naphthalen part (of which the C7 and N14 atoms are deviated by 0.164(3) and -0.171(3) Å respectively) and the remaining other ring atoms - excluding C3- linked in C7 and N14, and bent by 163° along the N14-C7 direction. The pyrano ring exhibits an envelope conformation with atom C3 deviated by 0.610(3) Å from the mean plane of the other five atoms. The two H atoms fixed at the chiral carbon atoms C1 and C2 appear in *cis* position, below the mean plane of this ring, respectively in bisecting and axial positions. Inversely, the two acetate substituents are situated above that mean plane, respectively in an axial position for the one linked to C1, with oxygen O21 at 1.365(2) Å, and in an equatorial position for the second linked to C2, with oxygen O22 at 0.432(2) Å. So, the absolute configuration of atoms C1 and C2 can be deduced unambiguously as *(S)*.

Molecular Pharmacology Fast Forward. Published on September 14, 2009 as DOI: 10.1124/mol.109.057554
This article has not been copyedited and formatted. The final version may differ from this version.

The pyramidal conformation of nitrogen atom N14 appears clearly with the methyl group C20 located at –1.897(4) Å from the mean plane of the molecule.

In the crystal packing, there are no π-π stacking interactions between the phenyl rings of the different molecules. Only contacts of types CH-π can be observed between the hydrogen atoms of the methyl group C15 (x,y,z) directed towards the phenyl ring [including atoms C9, C10 to C8a] of molecule (1-x, 0.5-y, 0.5+z) with distances: CH3-Cg centroid = 3.469 Å, H-Cg = 2.82 Å, angle C-H-Cg = 131°), strengthening the crystalline cohesion.

The configurations of the enantiomers of S29983-1 were deduced from the CD curves (Figure 1B) and compared with those obtained from S27589-1 and S27590-1 of known (*1S,2S*) and (*1R,2R*) configurations, respectively. Compound S70256-1, which exhibits a positive maximum at λ=356 nm, possesses the same *1S* configuration as S27589-1. Similarly, S70255-1 and S27590-1 exhibit a negative maximum reliable to the *1R* configuration.

Cytotoxicity and anti-tumor activities

We investigated the pharmacological properties of the different isomers (Scheme 1). For this purpose, both cytotoxic (Table 1) and *in vivo* antitumor activities (Figure 2) were studied. Both stereo-isomeric compounds were cytotoxic for the sensitive cell lines KB3-1, HCT116, MDA-MB-468 and NCI-H460 with IC50 in the same range, with the *1S*-isomers being slightly more potent (around 2-3 fold) than the *1R*-counterparts using both *cis*- and *trans*-series. Cell cycle analysis on L1210 cell line evidenced similar induced cell cycle effects using both compounds with a G2/M phase arrest at 1 µM evolving in S phase accumulation at higher concentrations (10 µM) (data not shown). Antitumor activities were measured on a C38 colon adenocarcinoma model. As evidenced in Figure 2A, S27589-1 is more active than the opposite *cis*-pure enantiomers S27590-1 on C38 model expressed as tumor growth (Figure

Molecular Pharmacology Fast Forward. Published on September 14, 2009 as DOI: 10.1124/mol.109.057554
This article has not been copyedited and formatted. The final version may differ from this version.

2A). As expected, the *cis*-racemate S23906-1 presents an intermediate profile. S23906-1, administered at 4 mg/kg twice to mice bearing NCI-H460 tumor, induced a prolongation of survival with a T/C of 241 %, this increase was significantly different from the control ($p = 0.002$) (Figure 2B). The mouse which survived on day 180, showed a tumor mass in the pleural space at the autopsy. The administration of 6 mg/kg of the enantiomers was toxic, early deaths were recorded with 5 and 6 mice who died after the first treatment with S27589-1 and S27590-1, respectively. The dose of 4 mg/kg was thus considered as the MTD for the two enantiomers, even if S27590-1 was more toxic than S27589-1, inducing one death on day 17 at 4 mg/kg. S27589-1 and S 27590-1, administered at 2 or 4 mg/kg, induced an increase in life span with maximal T/C of 229 % and 185 %, respectively. In the group treated by 2 mg/kg of S27590-1, two mice survived at the end of the experiment (day 180). The autopsy revealed that these two mice were not tumor-free. The increase in life span observed for the 4 mg/kg S27589-1 treated group was statistically different from the control with $p< 0.01$.

The efficacy of S27589-1 (4 mg/kg, T/C = 229 %) was superior to that of S27590-1 (4 mg/kg, T/C = 173 %), the differences in T/C being statistically different between the two groups ($p<0.01$). When administered at their MTD (4 mg/kg), S23906-1 and S27589-1 induced a T/C of 241 % and 229 %, respectively, showing that S23906-1 was slightly more active than S27589-1.

In order to understand why and how one of the two pure *cis*-enantiomers is more potent than the other, we investigated the mechanism of action of both *cis*- and *trans*- pure or racemate compounds.

Influence of the *cis*- or *trans*- isomeric position of racemate derivatives on DNA alkylation efficiency. The comparison of the DNA alkylation potencies of the various *cis*- or

Molecular Pharmacology Fast Forward. Published on September 14, 2009 as DOI: 10.1124/mol.109.057554
This article has not been copyedited and formatted. The final version may differ from this version.

trans-racemate derivatives of the di-acetate or mono-acetate forms of benzo[*b*]acronycine (Scheme 1) was investigated using a previously described assay (David-Cordonnier et al., 2002, 2003). In these initial studies, we focused on the *cis*-racemate forms of the mono- or di-acetate derivatives, S23906-1 and S28687-1, respectively, and clearly evidenced the DNA bonding rather than non-covalent binding of the interaction using sodium docedyl sulfate (SDS), NaCl or DNA competition experiments. Here, their respective *trans*-racemate homologues S29983-1 and S29850-1 were synthesized. A comparison of their covalent DNA bonding properties is presented in Figure 3. The *trans*-diacetylated racemate S29983-1 alkylates DNA with similar efficiency than the *cis*-diacetylated racemate S23906-1. By contrast, the *trans*-monoacetylated racemate S29850-1 totally fails to react with DNA. This result is in total agreement with previously published data demonstrating that a transesterification process is required to displace the acetate group from position *2* to the reactive position *1* of the *cis*-racemate compound S28687-1 (David-Cordonnier et al., 2004b). In the case of S29850-1, this transesterification process could not occur because of the high energy cost and this compound is consequently inactive. In the case of S29983-1, the departing acetate is present at the reactive position *1* and could potently react with guanines to form covalent DNA adducts.

DNA alkylation potency of the *cis*- or *trans*-pure enantiomers. Both pure enantiomers of the di-acetylated forms of benzo-*b*-acronycine were assessed for their covalent bonding to DNA using electromobility shift assays (EMSA). Figure 4A shows a comparison between the two pure *cis*- (S27589-1 and S27590-1, panel **A**) or *trans*- (S70255-1 and S70256-1, panel **B**) enantiomers for their ability to form a covalent complex with a radio-labeled 117 bp DNA fragment. All four isomers present comparable DNA alkylating efficiencies. A quantitative analysis of the migration delay upon DNA alkylation (Figure 4B) evidenced that DNA

Molecular Pharmacology Fast Forward. Published on September 14, 2009 as DOI: 10.1124/mol.109.057554
This article has not been copyedited and formatted. The final version may differ from this version.

alkylation efficiency, proportional to the retardation of the gel migration induced by the various compounds, is in the order S27590-1>S27589-1>S70255-1>S70256-1, corresponding to the acetate positions (*1R,2R)*>(*1S,2S)*>(*1R,2S)*>(*1S,2R)*. Therefore, the *cis*-isomers S27589-1 and S27590-1 are more potent than the *trans*-isomers S70255-1 and S70256-1. Similarly, compounds bearing the acetate group in the *1R* orientation (S27590-1 and S70255-1) are slightly more potent than their counterparts bearing the acetate in the *1S* orientation (S27589-1 and S70256-1) using the 117 bp DNA probe (Figure 4) or any other tested radio-labeled DNA fragments (Figure S1 and data not shown). The kinetics of reaction assessed using 50 µM of either compounds for a reaction time of up to 2 hours (Figure 5) reveal that the alkylation reaction is faster with the two *cis*-enantiomers (Figures 5A and 5C) than with the two *trans*-enantiomers (Figures 5B and 5C). A faster reaction was observed using the two *cis*-isomers compared to the *trans*-isomers. It is also more rapid with compounds bearing the acetate group at the *1R* than with the *1S* compounds. In terms of kinetics, the compounds rank in the order (*1R,2R)*>(*1S,2S)*>(*1R,2S)*>(*1S,2R)* which is consistent with the dose-dependent effects (Figure 3). The better reactivity of *1R* versus *1S* versions of the compound is in opposite correlation with the antitumor activity of the compounds for which the *1S* version is more potent than the *1R* (Figure 2).

Covalent binding to GSH

A direct correlation between DNA alkylation and cytotoxic/anti-tumor activities has been previously established for several chemical series of benzo-acronycine derivatives (David-Cordonnier et al., 2002; Doan Thi Mai et al., 2003; David-Cordonnier et al., 2004a; Nguyen et al., 2006). This is apparently not the case here. Therefore, we searched for an alternative explanation and, to this end, we investigated the reactivity against glutathione (GSH) which

Molecular Pharmacology Fast Forward. Published on September 14, 2009 as DOI: 10.1124/mol.109.057554
This article has not been copyedited and formatted. The final version may differ from this version.

has been considered as a potential detoxification process for S23906-1 and related molecules (David-Cordonnier et al., 2003).

All pure *cis*-enantiomers were tested for their bonding to glutathione (GSH). Both S27589-1 and S27590-1 were previously tested for their abilities to bond to glutathione using circular dichroism and mass spectrometry (David-Cordonnier et al., 2003). HPLC was used to separate the different reaction products and isomers. In a first instance, the racemate S23906-1 compound was incubated in the presence of GSH prior to the separation on a QS Uptispher 5-FT HPLC column and localization of the peaks corresponding to S23906-1 and metabolites or to the adducts bound to glutathione using the fluorescence properties of the benzo[*b*]acronycine core (Figure 6A). GSH alone was eluted from the column very early (3-4 min) and was detected by UV absorption at 280 nm (data not shown). Figure 6A evidences the formation of different adducts which elution from the column is more or less retarded. The di- or mono-acetylated and diol forms (open arrows) were assigned from a comparison of the retention profile of the mono-acetate S28687-1 and diol S23907-1 compounds (data not shown). Two series of double peaks were identified, coming out of the column at 6.2-8.5 and 17-19 min (double full arrows). Once the mobile phase was optimized, it was used to separate the adduct from the free compounds using an HPLC apparatus equipped with an ion-spray nebulizer coupled simple-quadrupole mass spectrometer. The di-acetate ([M+H] = 490), mono-acetate ([M+H] = 448) and diol ([M+H] = 406) derivatives were localized within the retention time attempted from fluorescence studies (blue arrows in Figure 6A). Two structurally different adducts could be obtained from alkylation of GSH by S23906-1: an adduct at [M+H] = 737 bearing an acetate group at position *2* of S23906-1 or an adduct at [M+H] = 695 bearing an OH group at position *2* obtained from the hydrolysis of S23906-1 as described previously (David-Cordonnier et al., 2002; 2003). From the HPLC separation, four peaks corresponding to the adduct at [M+H] = 737 were retained on the column and are

Molecular Pharmacology Fast Forward. Published on September 14, 2009 as DOI: 10.1124/mol.109.057554
This article has not been copyedited and formatted. The final version may differ from this version.

labeled ***a1***, ***a2***, ***b1*** and ***b2***. Similarly, two close double peaks corresponding to the adduct at [M+H] = 695 were found and labeled ***c1***, ***c2***, ***d1*** and ***d2*** (Figure 6B). HPLC separation of the adducts formed using the pure *cis*-enantiomers S27589-1 and S27590-1 discriminates between each generated adducts: peaks ***a1*** (8.4 min), ***b1*** (19.3 min), ***c1*** (6.9 min) and ***d1*** (8.0 min) could be attributed to the adduct generated from the *(1S,2S)* isoform S27589-1 (Figure 6C) whereas peaks ***a2*** (7.4 min), ***b2*** (19.9 min), ***c2*** (6.4 min) and ***d2*** (8.2 min) are attributed to the adduct generated from *(1R,2R)* counterpart S27590-1 (Figure 6D). From this study, it can be seen that both *cis*-isomers react with GSH in a similar manner. Interestingly, the formation of two kind of adducts of each type (adducts ***a*** or ***b*** for [M+H] = 737 and ***c*** or ***d*** for [M+H] = 595) is in agreement with the formation of an intermediate reactive carbocation generated after the release of the reactive acetate group in position *1* (Scheme 1). This carbocation has no asymmetric carbon and the resulting adduct could therefore be linked in the *1S* or *1R* orientation. Peaks ***a1*** and ***b1*** correspond to either *(1S,2S)* or *(1R,2S)* enantiomers whereas peaks ***a2*** and ***b2*** correspond to either *(1S,2R)* or *(1R,2R)* enantiomers bearing an acetate in position *2* (C2-acetate). A similar correlation could be established for peaks ***c1*** and ***d1*** and peaks ***c2*** and ***d2*** corresponding to the *(1S,2S)* or *(1R,2S)* and either *(1S,2R)* or *(1R,2R)* enantiomers in the series bearing a C2 –OH group. These data evidence the racemization of the adduct formed after the release of the reactive C1-acetate to form the reactive carbocation intermediate, as previously hypothesized (David-Cordonnier et al., 2002; 2004b).

Since both *cis*-enantiomers react in a similar manner with GSH and give similar orientation of GSH toward the core acronycine (the sole difference being the orientation of the acetate or -OH group), we looked at inhibition of the DNA alkylation efficiency with increasing concentrations of each of the *cis*-enantiomers in the presence of a fixed concentration of GSH. Each *cis*-enantiomers previously incubated with GSH present an important decrease in their DNA alkylation efficiency, with equal orders of magnitude (Figure S2). Therefore, both

Molecular Pharmacology Fast Forward. Published on September 14, 2009 as DOI: 10.1124/mol.109.057554
This article has not been copyedited and formatted. The final version may differ from this version.

compounds have similar reactivity profile on either DNA or GSH. As a consequence, GSH bonding could not be used as a criterion to select which of the enantiomer could be the best one for clinical use.

Alkylation of genomic DNA. In order to evaluate the influence of the stereo-isomeric position of the two acetate groups on DNA alkylation within cells, we exploited the fluorescence property of the benzo-acronycine core molecule to quantify the DNA adduct formation on extracted genomic DNA, as previously described (David-Cordonnier et al., 2002). The alkylation efficiency of genomic DNA of KB3-1 cells treated with increasing concentrations of the various derivatives was quantified using fluorescence excitation at 300 nm and emission at 510 nm. As shown in Figure 7, both compounds can enter the nucleus and alkylate genomic DNA. The *cis*-isomers (black symbols) are more potent than the *trans*-isomers (open symbols). These cellular results are fully consistent with gel shift data (Figures 3 and 5).

Drug-induced DNA destabilization. The ability of the various enantiomers to destabilize the DNA helix was evaluated using EMSA (Figure 8). Electrophoretic migration of reaction samples containing a radio-labeled 24-bp DNA oligonucleotide (designated XH-24) incubated with increasing amounts of diastereoisomers resulted in the creation of alkylated single-stranded DNA that migrates faster than the alkylated double-stranded DNA. Both *cis*-diacetates are more potent in destabilizing this small double strand DNA than any of the three *trans*-diacetates (both as racemate or pure enantiomers). Indeed, a 50 % denaturation is observed using 5 to 7.5 µM of the *cis*-derivatives versus 15-20 µM with the *trans*-isomers. Moreover, at 50 µM of any of the *cis*-enantiomers, all double-stranded alkylated DNA is converted into a single-stranded alkylated fragment whereas at this concentration, the double

Molecular Pharmacology Fast Forward. Published on September 14, 2009 as DOI: 10.1124/mol.109.057554
This article has not been copyedited and formatted. The final version may differ from this version.

stranded alkylated DNA (*ds-f*) remains observed in gels. This suggests that the *cis*-enantiomers are more potent in destabilizing the DNA helix than their relative *trans*-isomers. Such DNA destabilization ability was confirmed for either diastereoisomers using melting temperature studies. A decrease in the double strand DNA melting temperature was observed in the presence of any of the *cis*- or *trans*- pure enantiomers or racemate forms (data not shown).

To further differentiate the mechanism of alkylation by the various diastereoisomers, each molecule was incubated for 1 hour with a short hairpin oligonucleotide (HP-AGA) and subsequent alkylated products were separated on native polyacrylamide gel (Figure 9). The HP-AGA oligonucleotide was designed as a hairpin DNA with a single guanine in the stem portion providing a unique alkylation site within an AT-rich sequence. However, EMSA reveals two retarded bands in the presence of the racemate *cis*- (S23906-1) or *trans*-isomers (S29983-1). Interestingly, each pure enantiomers could only form one band, migrating at different level depending on the position of the acetate group relative to the core of the molecule. But each retarded band co-migrates with one or the other shifted position observed for the respective racemate compounds. Since only one adduct could be formed per oligonucleotide at the unique guanine site, this result suggests that different structural positioning of the adduct induces a different level of gel shift. Adduct formed with a link in the *1S* configuration (S27589-1) leads to a greater delay of migration than that formed through a bond at the *1R* orientation (S27590-1) of the core benzo-acronycine. One possible explanation is that the presence of the adduct in the different configurations induces a distinct orientation relative to the DNA helix and thus differently destabilizes the double-stranded stem of the hairpin to give single-stranded DNA. The higher level of retardation using the *1S* configuration correlates with the higher level of DNA opening using compounds bearing the reactive group in the *1S* configuration relatively to the *1R* configuration. This increase of the

Molecular Pharmacology Fast Forward. Published on September 14, 2009 as DOI: 10.1124/mol.109.057554
This article has not been copyedited and formatted. The final version may differ from this version.

delay of migration for a more potent DNA destabilizing compound is reinforced with the more important DNA retardation observed using the dicarbamate S29385-1 derivative previously evidenced as a stronger DNA destabilizing compound that S23906-1 (David-Cordonnier et al., 2005). Nuclease S1 digestion of the alkylated DNA fragment was performed to get an insight into the strength of each diastereoisomer to locally open the DNA helix. As presented in Figure 9, several nuclease S1 digestion sites could be identified using S23906-1. Similar cleavage sites are observed using the *trans*-isomer S29983-1 suggesting that they display the same mode of bonding. Interestingly, the two pure *cis*- or the two pure *trans*-compounds induce different cleavage sites, each of them being obtained using both racemate molecules. Therefore, cleavages sites obtained using S23906-1 represent an accumulation of that induced using S27589-1 and S27590-1.

Discussion

In the actual pharmacopoeia, the presence of an isomeric reactive group within a molecule requires further studies to assess the real medical potency of each of the isomers. Different stereoisomeric positions may give rise to different biological properties, pharmacological actions, side effects and metabolism, with first observation of Pasteur about (+)- but not (-)-tartrate being metabolized by *Penicilium glaucum* and first proofs evidenced by Puitti in 1886 on asparagine which (+)- or (-)-enantiomers present sweety taste or not, respectively. Each of the enantiomers could have (*i*) similar effects with nearly identical qualitative and quantitative effect, (*ii*) similar pharmacological effects but different concentration-response efficacies (*L*-(-)-verapamil is four-fold more active than *D*-(+)-verapamil at inhibiting MDR, Eliason et al., 1990), (*iii*) one could be active whereas the other is inactive ((+)-7β,8α-dihydroxy-9α,10α-epoxy-7,8,9,10-tetrahydrobenzo[*a*]pyrene presents an important tumorigenicity, whereas the other three optically pure isomers of the benzo[*a*]pyrene 7,8-diol-9,10-epoxides shows little or

Molecular Pharmacology Fast Forward. Published on September 14, 2009 as DOI: 10.1124/mol.109.057554
This article has not been copyedited and formatted. The final version may differ from this version.

no activity, Buening et al., 1978) or (*iv*) one is active while the other is toxic (Thalidomide whose *S*-form is assumed to be responsible for phocomelia in children born from thalidomide-treated mothers in the sixties, whereas the *R*-isomer was considered responsible of the anti-inflammatory and sedative effects, Melchert and List, 2007). The present study establishes the relevance of the absolute configuration of the di-acetylated form of benzo[*b*]acronycine on its cytotoxic and anti-tumor activities in correlation with its DNA alkylation and locally-induced DNA opening. The comparison of the cytotoxic and anti-tumor effects of both *cis*-enantiomers of S23906-1 indicates that the *1S*-isomer is slightly more potent than the *1R*-isomer. However, regarding the small difference, the resulting eudismic index is very close in terms of DNA alkylation and cytotoxic activities and we could not single out a real active eutomer form from an inactive distomer one. S23906-1 might belong to one of the first two groups defined above (*i* and *ii*).

In order to understand why the *1S*-isomer was slightly more potent than the *1R*-isomer, we conducted several biochemical experiments to evaluate *in vitro* DNA alkylation, kinetics of reaction as well as genomic DNA alkylation efficiencies. All experiments surprisingly evidence the *1R*-isomer as more potent than the *1S*-isomer in alkylating the DNA (Figures 4, 5 and 7). This contrasts with cytotoxic and *in vivo* data (Table 1 and Figure 2). Previous studies indicated a satisfactory correlation between (*in vitro* and *in cellulo*) DNA alkylation and the cytotoxic activities of different benzo[*b*]acronycine series (David-Cordonnier et al., 2002; Doan Thi Mai et al., 2003; David-Cordonnier et al., 2004a; Nguyen et al., 2006). But all previous data were obtained using the racemate but not the pure enantiomers. Identifying why the most potent DNA alkylating isomers are the worst cytotoxic ones is an important point to understand how those compounds act within cells and therefore for drug design and selection. We did not evidenced stereo-selective detoxification using GSH as an explanation for the DNA alkylation/cytotoxicity opposite correlation (Figure S2). However, a clear difference

Molecular Pharmacology Fast Forward. Published on September 14, 2009 as DOI: 10.1124/mol.109.057554
This article has not been copyedited and formatted. The final version may differ from this version.

between the *R*- or *S*-isomers is seen regarding their DNA destabilization potency (Figure 9). It is therefore postulated that different orientations of the fused ring relatively to the DNA axis, and dependent on the enantiomery of the adduct, could modulate the electronic distribution in the bases thus resulting in a change in the DNA local opening properties.

At the molecular level, another interesting conclusion of this work is that the *trans*-enantiomers form covalent binding to DNA with a slower kinetic compared to the *cis*-enantiomers (Figure 5). This is consistent with the hypothesis of the formation of an intermediate carbocation occurring after the release of the C1-acetate group. The release occurs faster in the presence of another acetate group in the vicinity of the leaving acetate. C1- and C2- acetate groups are positioned on the same side of the molecule relative to the planar organization of the core acronycine in the various *cis*-orientations thus facilitating the acetate departure. By contrast, the C2-acetate in both *trans*-configurations is spatially much more faraway from the C1-acetate, in correlation with a slower kinetic of carbocation formation through the release of the C1-acetate.

Overall, this study reinforces our idea that it is useful to study and compare the pure isomers of a racemate bioactive compound in order to evaluate their specific mode of action and identify potential consequences in terms of cellular activity and drug design. Even if no huge differences are observed using the two pure *cis*-isomers S27589-1 and S27590-1 defining an active and an inactive stereoisomer. The isomer inducing the wider local opening of the DNA helix is the one that presents the highest anti-tumor activity. Up to now, the potential correlation between anti-tumor activity and the opening of the DNA helix is not easy to explain but it is definitely a key point that must be controlled for future drug development and be further evaluated. Even if, at this stage, we cannot deny the assumption that the stereo-isomeric differences could also arise from a distinct metabolism of the various enantiomers in animal models, different DNA destabilization potencies seem to be a crucial DNA structural

Molecular Pharmacology Fast Forward. Published on September 14, 2009 as DOI: 10.1124/mol.109.057554
This article has not been copyedited and formatted. The final version may differ from this version.

change that may affect protein/DNA recognition by the cellular machineries as, for example, DNA repair (for recent review: Lenglet and David-Cordonnier, 2009). Such stereo-specific protein/DNA recognition was previously evidenced for platinated DNA adducts. In this case, cisplatin, but not transplatin, adducts are recognized by HMG proteins as part of the drug-induced DNA bent (Gelasco and Lippard, 1998) that perfectly fit the L-shape structure of HMG DNA binding domain (HMG-box) (Chow et al., 1994). Similarly, the Mut-S alpha (MSH2/MSH6 heterodimer) mismatch repair enzyme recognizes cisplatin but not transplatin crosslinks, probably as part as poor base stacking and base flipping generated by the cisplatin induced DNA bent (Fourier et al., 2003). Indeed, such distortions and constraints of the DNA are known to play a role in the initiation of the DNA lesions recognition by repair proteins (Fuxreiter et al., 2002; Yang et al., 2006). This stereo-selective binding of DNA repair proteins to a bulky DNA adduct was also recently evidenced for benzo[*a*]pyrene DNA adducts. BaP lesions are recognized by XPC, the "sensor" protein of the nucleotide excision repair machinery which associates with HR23B to initiate DNA repair (Moquet et al., 2007; Yuqin et al., 2009). Interestingly, BaP lesions are known to locally destabilize the DNA helix (Rodriguez et al., 2007). This destabilization occurs using the 5'-CG*GC sequence but not the 5'-CGG*C site (* correspond to the bulky adduct attached to the first or second G, respectively). In this latter, the BaP lesion strongly untwists the DNA resulting in a large bend but no destabilization of the DNA helix (Kropachev et al., 2009). Using cell-free human HeLa extracts, the destabilized DNA at 5'-CG*GC site is more rapidly excised than the bent DNA at 5'-CGG*C site. This suggests that, in the case of BaP, the recognition step of the lesion is less energetic and thus potentially more rapid when the DNA is already destabilized (5'-CG*GC site) from comparison with bent duplex DNA (5'-CGG*C site) (Kropachev et al., 2009). It will therefore be important to evaluate the DNA repair process and identify proteins

implicated in the recognition of DNA adducts formed upon alkylation using both S23906-1 and its various pure stereo-isomers.

Acknowledgments. Marie-Hélène David-Cordonnier thanks the Service de Spectrométrie de Masse de l'Université de Lille 2 (Drs Mostafa Kouach and Gilbert Briand) for access to and expertise in HPLC-coupled simple-quadrupole mass spectrometer API 3000 equipment, Nicole Wattez for expert technical advices in HPLC separation.

References

Blessington B (1997) Ethambutol and tuberculosis, a neglected and confused chiral puzzle. *Chemical Analysis* (Impact of Stereochemistry on Drug Development and Use) **142:** 235-261.

Brum-Bousquet M, Mitaku S, Skaltsounis AL, Tillequin F, and Koch M (1988) Acronycine epoxide : a new acridone alkaloid from several sarcomelicope species. *Planta Med* **54:** 470-471.

Buening MK, Wislocki PG, Levin W, Yagi H, Thakker DR, Akagi H, Koreeda M, Jerina DM,, and Conney AH (1978) Tumorigenicity of the optical enantiomers of the diastereomeric benzo[*a*]pyrene 7,8-diol-9,10-epoxides in newborn mice: exceptional activity of (+)-7ß,8-dihydroxy-9,10-epoxy-7,8,9,10-tetrahydrobenzo[*a*]pyrene. *Proc Natl Acad Sci USA* **75:** 5358-5361.

Chow CS, Whitehead JP, and Lippard SJ (1994) HMG domain proteins induce sharp bends in cisplatin-modified DNA. *Biochemistry* **33:** 15124-15130.

Cimino P, Bifulco G, Riccio R, Gomez-Paloma L, and Barone V (2006) On the role of stereo-electronic effects in tuning the selectivity and rate of DNA alkylation by duocarmycins. *Org Biomol Chem* **4 :** 1242-1251.

Costes N, Le Deit H, Michel S, Tillequin F, Koch M, Pfeiffer B, Renard P, Léonce S, Guilbaud N, Kraus-Berthier L, Atassi G, and Pierré A (2000) Synthesis and cytotoxic and antitumor activity of benzo[*b*]pyrano[3,2-*h*]acridin-7-one analogues of acronycine. *J Med Chem* **43:** 2395-2402.

David-Cordonnier MH, Laine W, Lansiaux A, Kouach M, Briand G, Pierré A, Hickman JA, and Bailly C (2002) Alkylation of guanine in DNA by S23906-1, a novel potent antitumor compound derived from the plant alkaloid acronycine. *Biochemistry* **41:** 9911-9920.

David-Cordonnier MH, Laine W, Joubert A, Tardy C, Goossens JF, Kouach M, Briand G, Doan Thi Mai H, Michel S, Tillequin F, Koch M, Léonce S, Pierré A, and Bailly C (2003) Covalent binding to glutathione prevents DNA alkylation by the benzoacronycine antitumor agent S23906-1. *Eur J Biochem* **270:** 2848-2859.

David-Cordonnier MH, Laine W, Gaslonde T, Michel S, Tillequin F, Koch M, Léonce S, Pierré A, and Bailly C (2004a) Design of novel antitumor DNA alkylating agents: the benzacronycine series. *Current Medicinal Chemistry-Anti-Cancer Agents* **4:** 83-92.

David-Cordonnier MH, Laine W, Kouach M, Briand G, Vezin H, Gaslonde T, Michel S, Doan Thi Mai H, Tillequin F, Koch M, Léonce S, Pierré A, and Bailly C (2004b) A transesterification reaction is implicated in the covalent binding of benzo[*b*]acronycine anticancer agents with DNA and glutathione. *Bioorg Med Chem* **12:** 23-29.

David-Cordonnier MH, Laine W, Lansiaux A, Rosu F, Colson P, de Pauw E, Michel S, Tillequin F, Koch M, Hickman JA, Pierré A, and Bailly C (2005) Covalent binding of antitumor benzoacronycines to double stranded DNA induces helix opening and the formation of single stranded DNA: A novel DNA binding approach. *Mol Cancer Ther* **4:** 71-80.

David-Cordonnier MH, Casely-Hayford MA, Kouach M, Briand G, Patterson LH, Bailly C, and Searcey M (2006) Stereoselectivity and sequence specificity of the azinomycin epoxide. *Chembiochem* **7:** 1658-1661.

Doan Thi Mai H, Gaslonde T, Michel S, Tillequin F, Koch M, Bongui JB, Elomri A, Seguin E, Pfeiffer B, Renard P, David-Cordonnier MH, Tardy C, Laine W, Bailly C, Kraus-Berthier L, Léonce S, Hickman JA, and Pierré A (2003) Structure activity relationships and mechanism of action of antitumor benzo[3,2-*h*]acridin-7-one analogs of acronycine. *J Med Chem* **46:** 3072-3082.

Eliason JF, Ramuz H, and Kaufmann F (1990) Human multi-drug-resistant cancer cells exhibit a high degree of selectivity for stereoisomers of verapamil and quinidine. *Int J Cancer* **46:** 113-117.

Fourrier L, Brooks P, and Malinge JM (2003) Binding discrimination of MutS to a set of lesions and compound lesions (base damage and mismatch) reveals its potential role as a cisplatin-damaged DNA sensing protein. *J Biol Chem* **278:** 21267-21275.

Fuxreiter M, Luo N, Jedlovszky P, Simon I, and Osman R (2002) Role of base flipping in specific recognition of damaged DNA by repair enzymes. *J Mol Biol* **323:** 823-834.

Gelasco A and Lippard SJ (1998) NMR solution structure of a DNA dodecamer duplex containing a *cis*-diammineplatinum(II) d(GpG) intrastrand cross-link, the major adduct of the anticancer drug cisplatin. *Biochemistry* **37:** 9230-9239.

Gower AJ, Noyer M, Verloes R, Gobert J, and Wülfert E (1992) Ucb L059, a novel anti-convulsant drug: pharmacological profile in animals. *Eur J Pharmacol* **222:** 193-203.

Guilbaud N, Léonce S, Tillequin F, Koch M, Hickman JA, and Pierré A (2002) Acronycine derivatives as promising antitumor agents. *Anticancer Drugs* **13:** 445-449.

Kluza J, Lansiaux A, Wattez N, Hildebrand MP, Léonce S, Pierré A, Hickman JA, and Bailly C (2002) Induction of apoptosis in HL-60 leukemia and B16 melanoma cells by the acronycine derivative S23906-1. *Biochem Pharmacol* **63:** 1443-1452.

Kroemer HK, Turgeon J, Parker RA, and Roden DM (1989) Flecainide enantiomers: disposition in human subjects and electrophysiologic actions. *Clin Pharmacol Ther* **46**, 584-590.

Kropachev K, Kolbanovskii M, Cai Y, Rodríguez F, Kolbanovskii A, Liu Y, Zhang L, Amin S, Patel D, Broyde S, and Geacintov NE (2009) The sequence dependence of human nucleotide excision repair efficiencies of benzo[*a*]pyrene-derived DNA lesions: Insights into the structural factors that favor dual incisions. *J Mol Biol* **386:** 1193-1203.

Lenglet G., David-Cordonnier M.-H. (2009) Drug/DNA interaction: DNA-destabilizing agents, a novel approach in cancer treatment? *Rec. Adv. Nucl. Acids Res., R.M. Mohan editor*. **3:** 35-53.

Leonce S, Pierré A, Anstett M, Perez V, Genton A, Bizzari JP, and Atassi G (1992) Effects of a new triazinoaminopiperidine derivative on adriamycin accumulation and retention in cells displaying P-glycoprotein-mediated multidrug resistance. *Bio-Chem Pharmacol* **44:** 1707-1715.

Léonce S, Pérez V, Lambel S, Peyroulan D, Tillequin F, Michel S, Koch M, Pfeiffer B, Atassi G, Hickman JA, and Pierré A (2001) Induction of cyclin E and inhibition of DNA synthesis by the novel acronycine derivative S23906-1 precede the irreversible arrest of tumor cells in S phase leading to apoptosis. *Mol Pharmacol* **60:** 1383-1391.

Léonce S, Kraus-Berthier L, Golsteyn R, David-Cordonnier MH, Tardy C, Lansiaux A, Poindessous V, Larsen AK, and Pierré A (2006) Generation of replication-dependent double-strand breaks by the novel N2-G-alkylator S23906-1. *Cancer Res* **66:** 7203-7210.

Levin W, Chang RL, Wood AW, Thakker DR, Yagi H, Jerina DM, and Conney AH (1986) Tumorigenicity of optical isomers of the diastereomeric bay-region 3,4- diol-l,2-epoxides of benzo[*c*]phenanthrene in murine tumor models. *Cancer Res* **46:** 2257-2261.

Magyar J, Rusznak Z, Harasztosi C, Kortvély A, Pacher P, Banyasz T, Pankucsi C, Kovacs L, Szûcs G, Nanasi PP, and Kecskeméti V(2003) Differential effects of fluoxetine enantiomers in mammalian neural and cardiac. *Int J Mol Med* **11:** 535-542.

Melchert M and List A (2007) The thalidomide saga. *Int J Biochem Cell Biol* **39:** 1489-1499.

Mocquet V, Kropachev K, Kolbanovskiy M, Kolbanovskiy A, Tapias A, Cai Y, Broyde S, Geacintov NE, and Egly JM (2007) The human DNA repair factor XPC-HR23B distinguishes stereoisomeric benzo[a]pyrenyl-DNA lesions. *EMBO J* **26:** 2923-2932.

Nguyen TM, Sittisombut C, Lallemand MC, Michel S, Koch M, Tillequin F, Mazinghien R, Lansiaux A, David-Cordonnier MH, Pfeiffer B, Kraus-Berthier L, Léonce S, Hickman JA, and Pierré A (2006) Synthesis, cytotoxic and antitumor activity and mechanism of action of benzo[*a*]pyrano[3,2-*h*]acridin-7-one analogs of acronycine. *J Med Chem* **49:** 3383-3394.

Pommier Y, Kohlhagen G, Bailly C, Waring M, Mazumder A, and Kohn KW (1996) DNA sequence- and structure-selective alkylation of guanine N2 in the DNA minor groove by ecteinascidin 743, a potent antitumor compound from the Caribbean tunicate Ecteinascidia turbinata. *Biochemistry* **35:** 13303-13309.

Rodríguez FA, Cai Y, Lin C, Tang Y, Kolbanovskiy A, Amin S, Patel DJ, Broyde S, and Geacintov NE (2007) Exocyclic amino groups of flanking guanines govern sequence-dependent adduct conformations and local structural distortions for minor groove-

aligned benzo[*a*]pyrenyl-guanine lesions in a GG mutation hotspot context. *Nucleic Acids Res* **35:** 1555-1568.

Sheldrick GM (1990) SHELXS86. *Acta Cryst A* **46:** 467-473.

Sheldrick GM (1997) SHELX97. Program for the Refinement of Crystal Structures, Univ. of Göttingen, Germany.

Spek AL (2003) PLATON. *J Appl Cryst* **36:** 7-13.

Takahashi H and Echizen H (2001) Pharmacogenetics of warfarin elimination and its clinical implications. *Clin Pharmacokinet* **40:** 587–603.

Wani MC, Nicholas AW, and Wall ME (1987) Plant antitumor agents. 28. Resolution of a key tricyclic synthon, 5'(*RS*)-1,5-dioxo-5'-ethyl-5'-hydroxy-2'*H*,5'*H*,6'*H*-6'-oxopyrano[3',4'-*f*]delta 6,8-tetrahydro-indolizine: total synthesis and antitumor activity of 20(*S*)- and 20(*R*)-camptothecin. *J Med Chem* **30:** 2317-2319.

Williams ML and Wainer IW (1999) Cyclophosphamide versus ifosfamide: to use ifosfamide or not to use, that is the three-dimensional question. *Curr Pharm Des* **5:** 665-672.

Yang W (2006) Poor base stacking at DNA lesions may initiate recognition by many repair proteins. *DNA Repair (Amst)* **5:** 654-666.

Yuqin C, Dinshaw JP, Nicholas EG, and Suse B (2009) Differential nucleotide excision repair susceptibility of bulky DNA adducts in different sequence contexts: Hierarchies of recognition signals. *J Mol Biol* **385:** 30-44.

Molecular Pharmacology Fast Forward. Published on September 14, 2009 as DOI: 10.1124/mol.109.057554
This article has not been copyedited and formatted. The final version may differ from this version.

Footnotes.

a)

This work was supported by grants to MHDC from the Institut pour la Recherche sur le Cancer de Lille (IRCL) and the Ligue Nationale Contre le Cancer, Comité du Nord.

b)

Dr Marie-Hélène David-Cordonnier

INSERM-U837 - Centre de Recherches Jean-Pierre Aubert (JPARC)

Team-4 "Molecular and Cellular Targeting for Cancer Treatment"

Institut pour la Recherche sur le Cancer de Lille, Place de Verdun

F-59045 Lille, France

Tel: (+33) 3 20 16 92 23/20

Fax: (+33) 3 20 16 92 29

E-mail: marie-helene.david@inserm.fr

c)

C.B. present address: Centre de Recherche en Oncologie Expérimentale, Institut de Recherche Pierre Fabre, 3 rue des satellites, F-31140 Toulouse, France.

Molecular Pharmacology Fast Forward. Published on September 14, 2009 as DOI: 10.1124/mol.109.057554
This article has not been copyedited and formatted. The final version may differ from this version.

Legend of schemes

Scheme 1: Structure of the various compounds. The different *cis*- and *trans*-racemate and pure enantiomers of the diacetate derivative of the benzo[*b*]acronycine, the *cis*- and *trans*-racemate of the mono-acetylated form as well as the *cis*-racemate of the dicarbamate derivatives are presented. The asymmetric carbons bearing the reactive groups are presented as stars. Identical six-pointed stars "*" refer to asymmetric carbons bearing the acetate (S23906-1) or carbamate (S29385-1) groups in identical orientations. The two different five-pointed stars represent opposite orientation of the acetate groups bore by S29983-1 at positions *1* or *2*.

Scheme 2: Bromination reaction and structure of the di-bromide (***a***) and mono-bromide (***b***) substituted compounds.

Legends of figures

Figure 1: Determination of the (*S,R)* configurations of the various isomers. A. Ortep drawing of the (+)*cis*-1,2-diacetoxy-5,13-dibromo-6-methoxy-3,3,14-trimethyl-1,2,3,14-tetrahydro-7*H*-benzo[*b*]pyrano[3,2-*h*]acridin-7-one (drawn with program *PLATON*) (Spek, 2003) giving the atomic labeling. Displacement ellipsoids are shown at the 30% probability level. **B.** CD curves of the four stereoisomers of 1,2-diacetoxy-6-methoxy-3,3,14-trimethyl-1,2,3,14-tetrahydro-7H-benzo[b]pyrano[3,2-h]acridin-7-one.

Figure 2: Antitumor activities of the various *cis*-benzo-*b*-acronycine diacetylated enantiomers on C38 colon carcinoma model and survival studies after treatment on NCI-H460 non-small-cell lung carcinoma. A. The volume of C38 tumor xenografts

Molecular Pharmacology Fast Forward. Published on September 14, 2009 as DOI: 10.1124/mol.109.057554
This article has not been copyedited and formatted. The final version may differ from this version.

implanted at day 0 was quantified twice a week in seven mice per sub-group. Treatment using 1, 2, 3 or 4 mg/kg of the racemate S23906-1 or any of the two pure *cis*-enantiomers S27589-1 and S27590-1 was performed at day 12 and 22 after implantation. Untreated mice and mice injected with equivalent volume of cremophor ELP/EtOH as a solvent were used as controls. **B.** Survival of mice treated with increasing amounts of S27589-1 or S27590-1 from comparison with mice treated with a fixed amount of S23906-1 or untreated mice. Treatments started 7 days post NCI-H460 non-small-cell lung carcinoma cell injection (*i.pl.*).

Figure 3: Gel shift retardation of DNA by *trans*-racemate of the mono-OH-mono-acetatylated or di-acetylated forms of benzo[*b*]acronycine. Increasing concentrations from 2 to 50 µM of the racemate *trans*-mono-acetate (S29850-1) or *trans*-di-acetate (S29983-1) were incubated with a 117 bp radio-labeled DNA fragment for 16 hours from comparison with the racemate *cis*-mono-acetate (S28687-1), *cis*-diacetate (S23906-1) or the *cis*-diol (S23907-1). Free (*f*) and alkylated (bound, *b*) DNAs were resolved on a 10 % polyacrylamide gel.

Figure 4: Gel shift retardation of DNA by the various pure enantiomers of the diacetate derivative of benzo[*b*]acronycine. A. Increasing concentrations from 1 to 50 µM of the various *cis*- and *trans*- pure enantiomers were incubated with a 117 bp radio-labeled DNA fragment for 16 hours. Free (*f*) and alkylated (bound, *b*) DNAs were resolved on a 10 % polyacrylamide gel. **B.** Quantification of the percentage of migration using alkylated DNA from comparison with the maximum migration distance using free DNA (lanes DNA). The percentage of migration $\Delta L = L_{Alk} / L_{DNA}$ where L_{Alk} and L_{DNA} corresponds to the medium distance of the band from the wells of the gel for alkylated DNA samples or control non-alkylated DNA, respectively.

Molecular Pharmacology Fast Forward. Published on September 14, 2009 as DOI: 10.1124/mol.109.057554
This article has not been copyedited and formatted. The final version may differ from this version.

Figure 5: Kinetic measurements of the four diastereoisomers of the diactetylated compound. A. Electromobility shift assays of the four diastereoisomers (50 µM each) incubated with the radio-labeled DNA for the indicated time (min) prior to be subjected to electrophoresis. Free (*f*) and alkylated (bound, *b*) DNAs were resolved on a 10 % polyacrylamide gel. **B.** Quantification of the percentage of migration $\Delta L = L_{Alk} / L_{DNA}$ as described in Figure 5.

Figure 6: HPLC separation and mass spectra analysis of the adduct formed upon bonding of S23906-1 or its two pure *cis*-enantiomers on GSH. A. HPLC separation profile for 50 µM of S23906-1 incubated for 24H alone (upper panel) or with an equal concentration of GSH (lower panel) is measured using fluorescence properties of the benzo-*b*-acronycine core of S23906-1 (λ_{ex} = 354 nm; λ_{em} = 510 nm). Open arrows localized the di-acetylated, mono-acetylated and diol forms. Two series of double peaks that appears after incubation with GSH are exemplified with double full arrows. HPLC-EI/MS was performed using GSH incubated for 24 H with S23906-1 (**B**), S27589-1 (**C**) or S27590-1 (**D**). The retention time for adducts at m/z [M+H] = 737 or at m/z [M+H] = 695 are presented in each panels.

Figure 7: Detection of DNA adducts from the *cis*- or *trans*-racemate or pure enantiomers of the di-acetate in genomic DNA. KB3-1 cells were treated using 1, 2.5, 5, 7.5, 10 and 15 µM of the various tested drugs for 24 h. The fluorescence (λ_{ex} = 300 nm; λ_{em} = 510 nm) of identical concentrations of extracted genomic DNA is plotted over drug concentration. This graph is a representative quantification of two independent experiments.

Molecular Pharmacology Fast Forward. Published on September 14, 2009 as DOI: 10.1124/mol.109.057554
This article has not been copyedited and formatted. The final version may differ from this version.

Figure 8: Gel shift analysis of the DNA strand scission in the presence of the various racemate or pure enantiomers of the diacetate compound. Either *cis*- (**A**) or *trans*- (**B**) compounds were incubated at the concentrations ranging from 1 to 50 µM, as specified on the top of the lanes, with a radio-labeled double-stranded XH-24 bp oligonucleotide for 2 hours at 37°C. Electrophoretic migration reveals different radio-labeled bands identified using arrows: *ds-f*, free double-stranded oligonucleotide; *ds-b*, alkylated (bound) double-stranded oligonucleotide; *ss-f*, free single-stranded oligonucleotide; *ds-b*, alkylated (bound) single-stranded oligonucleotide.

Figure 9: Drug induced DNA-destabilization. A. DNA alkylation within a short hairpin oligonucleotide. EMSA was performed by incubating the short 22-mer oligonucleotide with a 9 bp stem containing a single guanine (*) surrounded by two adenine bases (HP-AGA) with 50 µM of various racemate or enantiomers of *cis*- or *trans*- diacetate compound or the racemate *cis*-dicarbamate S29385-1 as a control. **B.** Nuclease S1 digestion of single-stranded DNA generated after benzo-acronycine alkylation of the DNA. The various di-acetylated forms of the benzo-*b*-acronycine core (µM) were incubated for 1H with the radio-labeled 117-bp DNA fragment prior to digestion of the DNA at single-stranded positions by addition of nuclease S1 and subsequent incubation. The generated DNA fragments were resolved on a 10 % native polyacrylamide gel under denaturing conditions. Free and bound DNA fractions are localized as "*f*" and "*b*" forms. Localization of the drug-induced S1 nuclease cleavage sites ("*NS1*") are exemplified by arrows. Nuclease S1 sites generated a position similar to that obtained in the presence of the pure enantiomers bearing a reactive acetate at the *1S* position (S27589-1 and S70256-1) are localized using a dashed arrow whereas that obtained in the presence of their respective isomers bearing the acetate leaving group at position *1R* are presented using a plain shaft arrow.

Molecular Pharmacology Fast Forward. Published on September 14, 2009 as DOI: 10.1124/mol.109.057554
This article has not been copyedited and formatted. The final version may differ from this version.

Table 1. Cytotoxicity measurements of the various racemate and pure enantiomers of the benzo-*b*-acronycine diacetates.

Cytotoxicity											
	Cell line	**S23906-1**	**sem**[a]	**n**[b]	**S27589-1**	**sem**[a]	**n**[b]	**S27590-1**	**sem**[a]	**n**[b]	**Ratio S27590/S27589**
IC_{50} (µM)	**KB3-1**	0.095	0.017	6	0.115	0.018	6	0.227	0.076	9	2
	HCT116	0.199	0.022	7	0.174	0.025	3	0.472	0.081	3	2.7
	HT29	1.48	0.12	10	1.21	0.18	4	1.65	0.32	4	1.4
	MDA-MB-468	0.033	0.007	3	0.038	0.009	3	0.117	0.041	3	3.1
	NCI-H460	0.22	0.03	3	0.28	0.01	3	0.59	0.067	3	2.1
	NCI-H69	0.047	0.014	3	0.047		2	0.072		2	1.5
	Cell line	**S29983-1**			**S70255-1**			**S70256-1**			**Ratio S70255/S70256**
	KB3-1	0.132	0.012	3	0.237	0.028	3	0.093	0.018	3	2.5

[a] Standard deviation; [b] number of independent experiments performed in triplicate.

Molecular Pharmacology Fast Forward. Published on September 14, 2009 as DOI: 10.1124/mol.109.057554
This article has not been copyedited and formatted. The final version may differ from this version.

Scheme 1

Acronycine

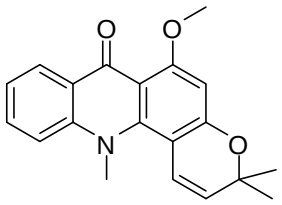

Benzo[*b*]acronycine

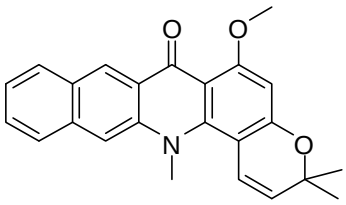

S23907-1

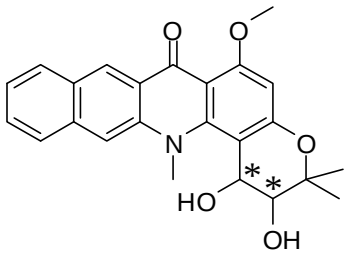

S23906-1

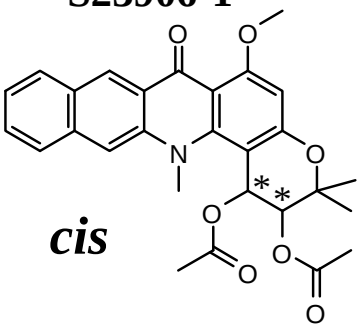

cis

S27589-1

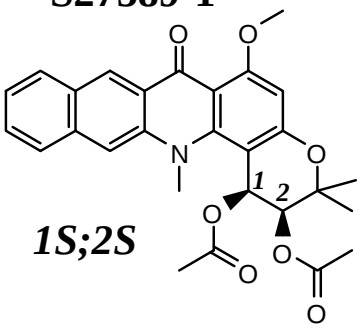

1S;2S

S27590-1

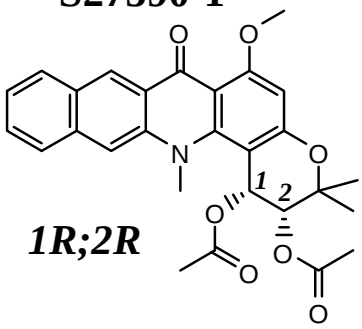

1R;2R

S29983-1

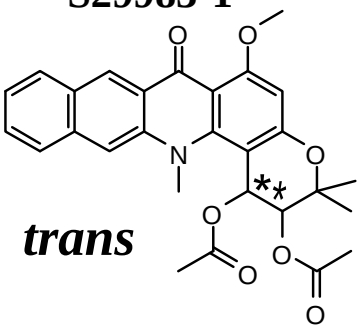

trans

S70256-1

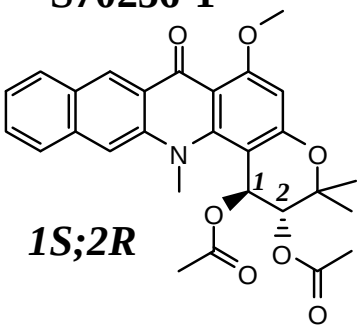

1S;2R

S70255-1

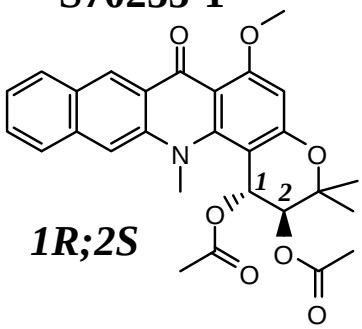

1R;2S

S28687-1

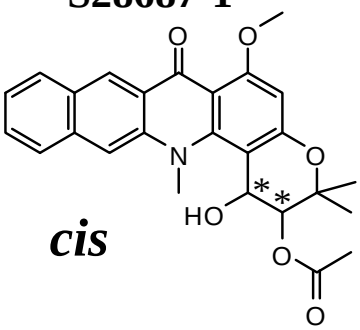

cis

S29850-1

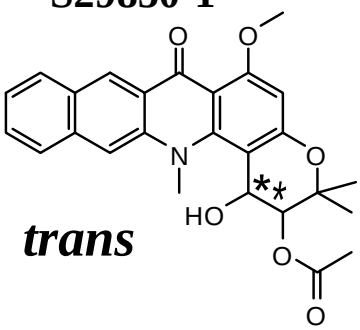

trans

S29385-1

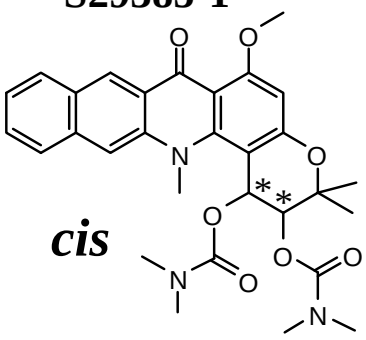

cis

Molecular Pharmacology Fast Forward. Published on September 14, 2009 as DOI: 10.1124/mol.109.057554
This article has not been copyedited and formatted. The final version may differ from this version.

Scheme 2

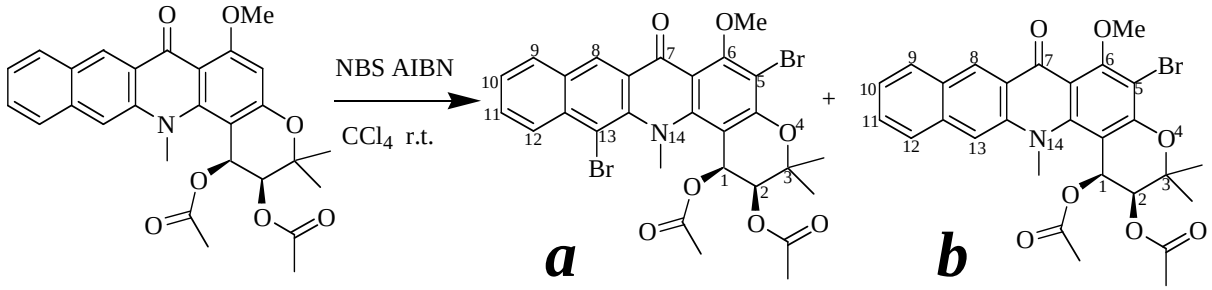

Molecular Pharmacology Fast Forward. Published on September 14, 2009 as DOI: 10.1124/mol.109.057554
This article has not been copyedited and formatted. The final version may differ from this version.

Figure 1

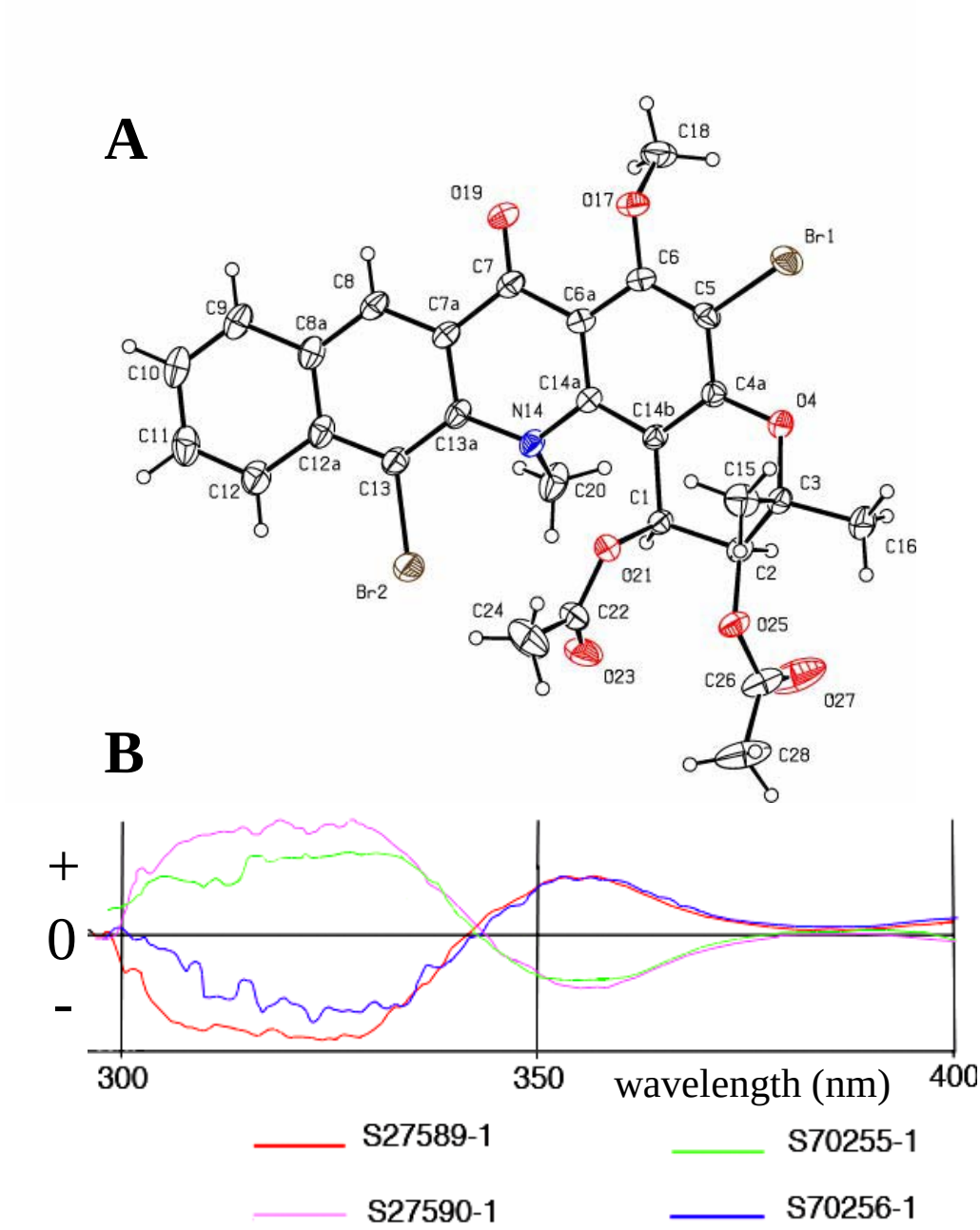

Molecular Pharmacology Fast Forward. Published on September 14, 2009 as DOI: 10.1124/mol.109.057554
This article has not been copyedited and formatted. The final version may differ from this version.

Figure 2

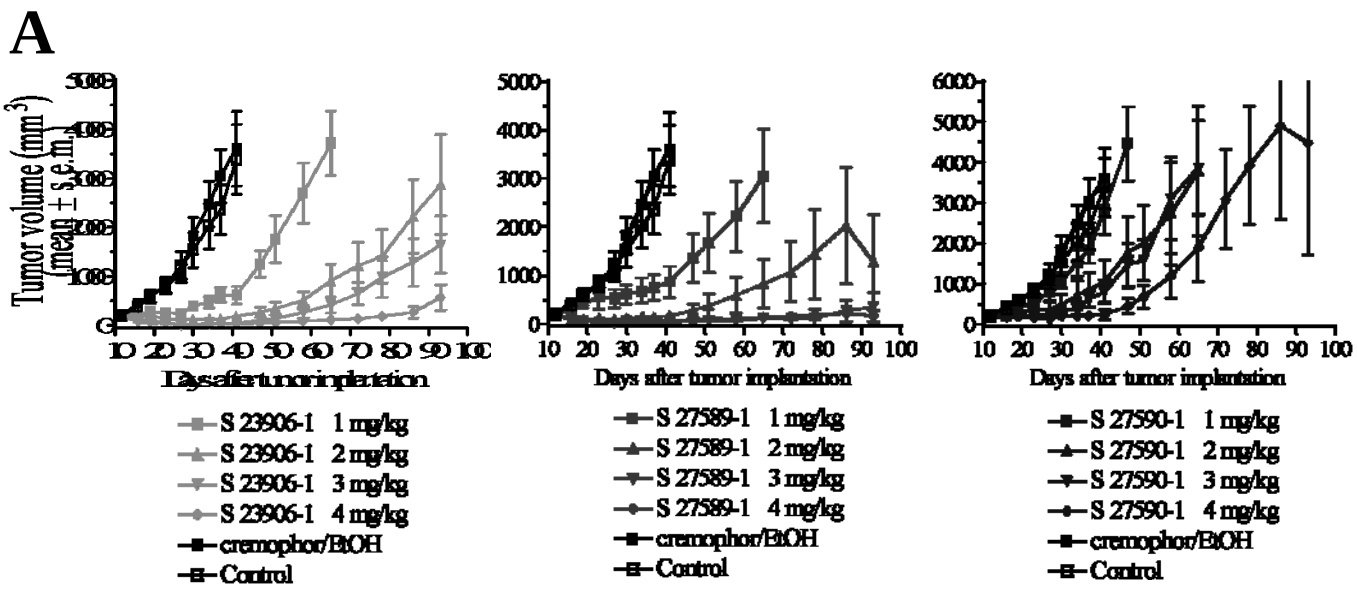

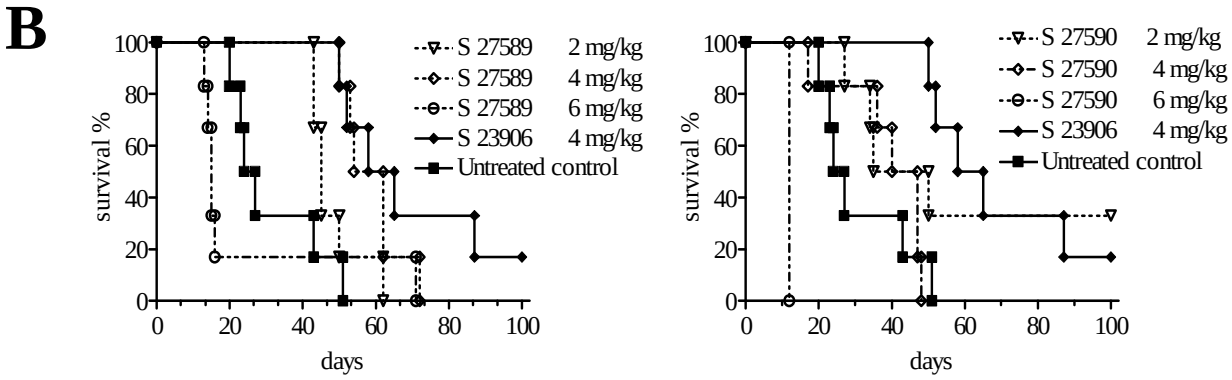

Molecular Pharmacology Fast Forward. Published on September 14, 2009 as DOI: 10.1124/mol.109.057554
This article has not been copyedited and formatted. The final version may differ from this version.

Figure 3

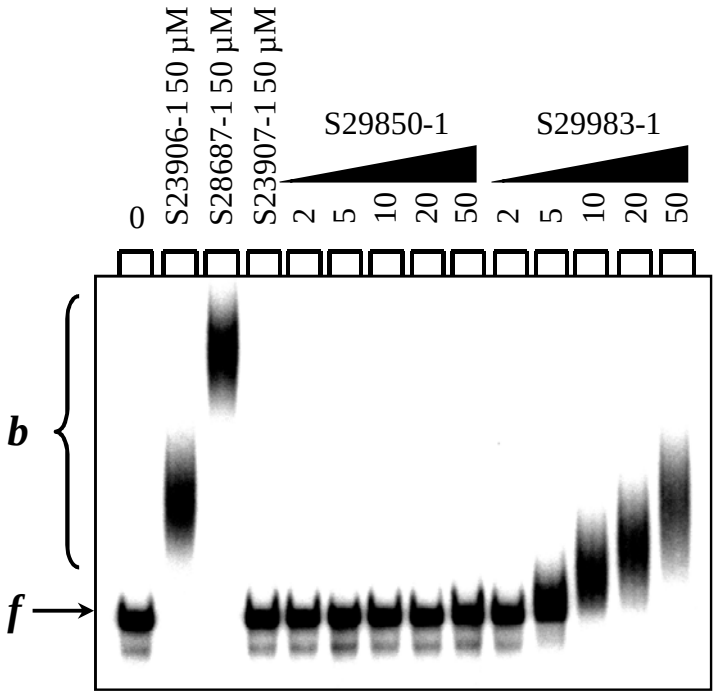

Molecular Pharmacology Fast Forward. Published on September 14, 2009 as DOI: 10.1124/mol.109.057554
This article has not been copyedited and formatted. The final version may differ from this version.

Figure 4

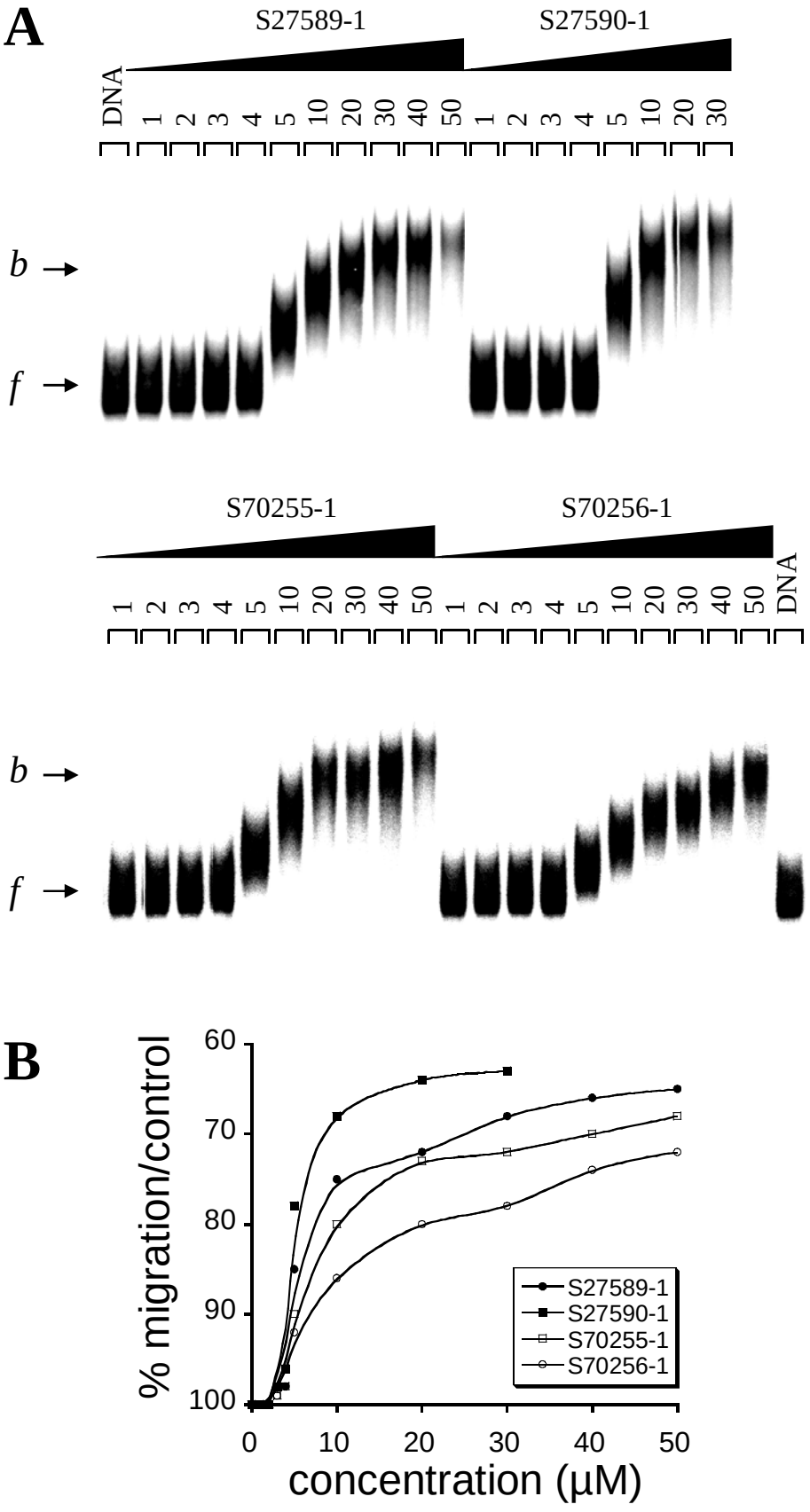

Molecular Pharmacology Fast Forward. Published on September 14, 2009 as DOI: 10.1124/mol.109.057554
This article has not been copyedited and formatted. The final version may differ from this version.

Figure 5

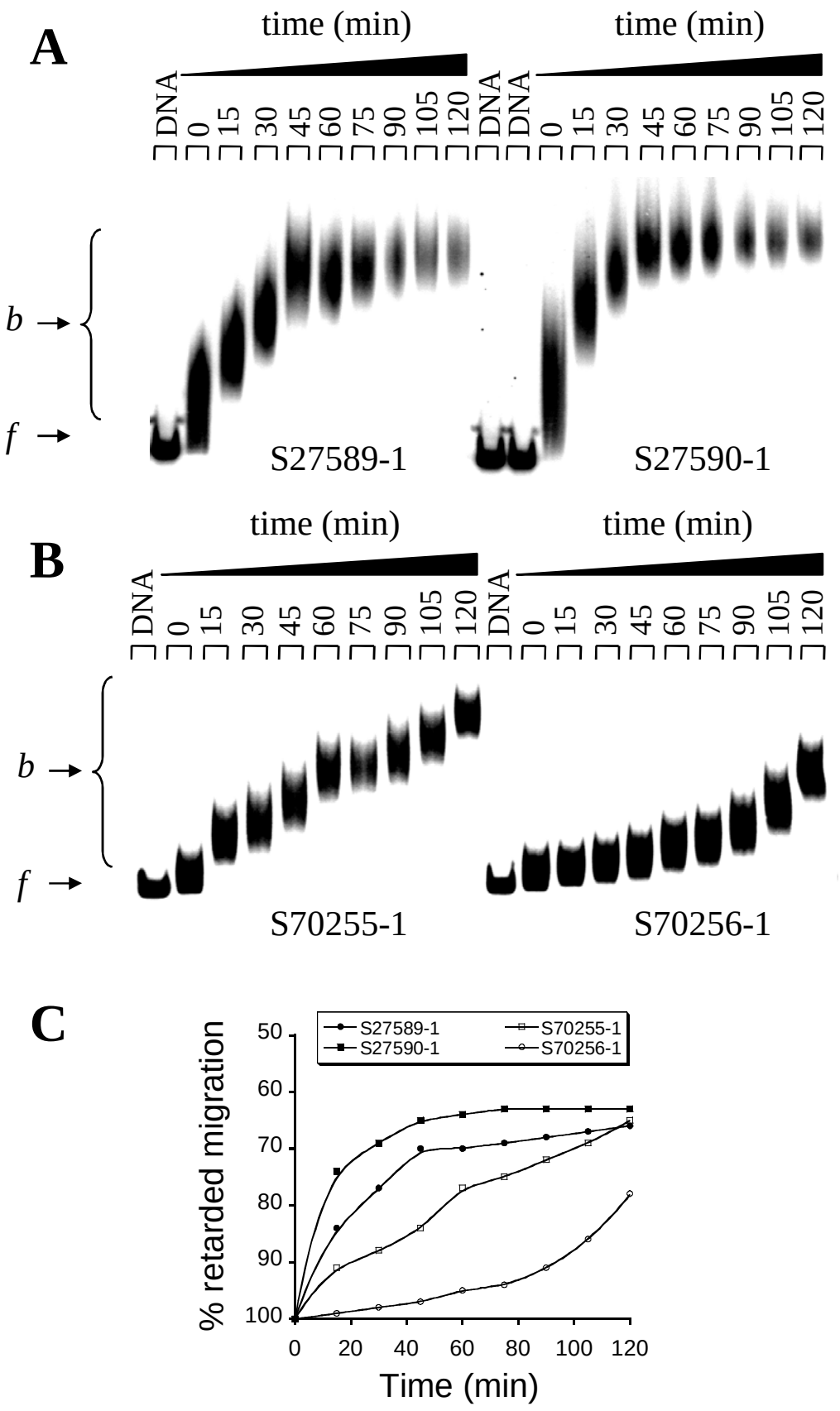

Molecular Pharmacology Fast Forward. Published on September 14, 2009 as DOI: 10.1124/mol.109.057554
This article has not been copyedited and formatted. The final version may differ from this version.

Figure 6

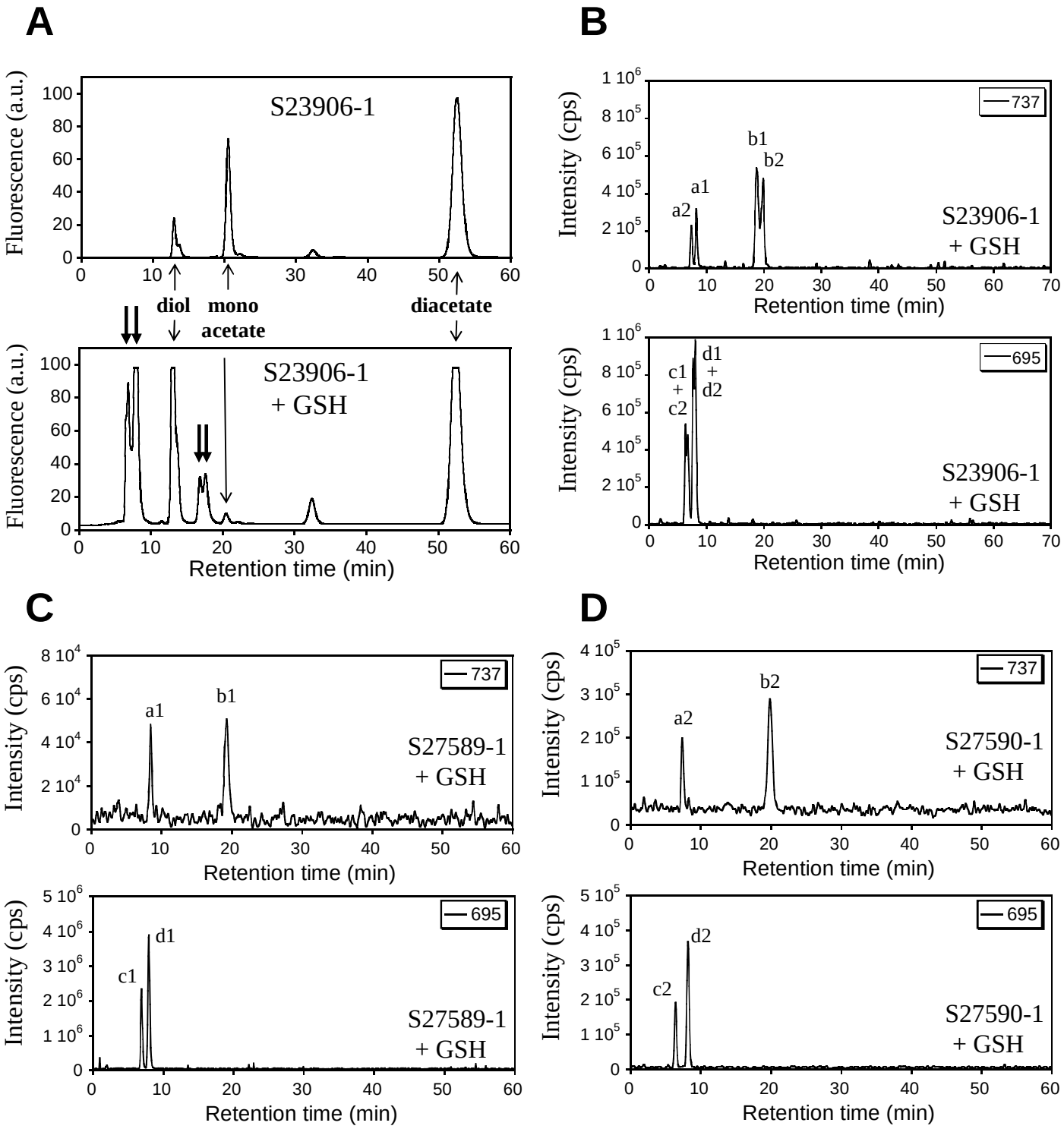

Molecular Pharmacology Fast Forward. Published on September 14, 2009 as DOI: 10.1124/mol.109.057554
This article has not been copyedited and formatted. The final version may differ from this version.

Figure 7

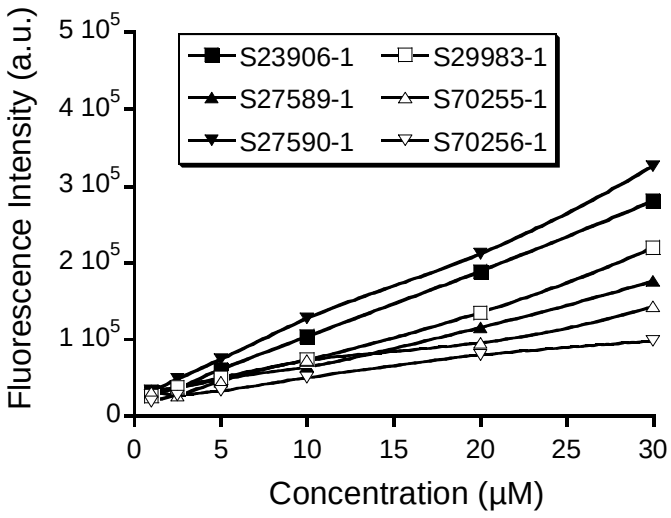

Molecular Pharmacology Fast Forward. Published on September 14, 2009 as DOI: 10.1124/mol.109.057554
This article has not been copyedited and formatted. The final version may differ from this version.

Figure 8

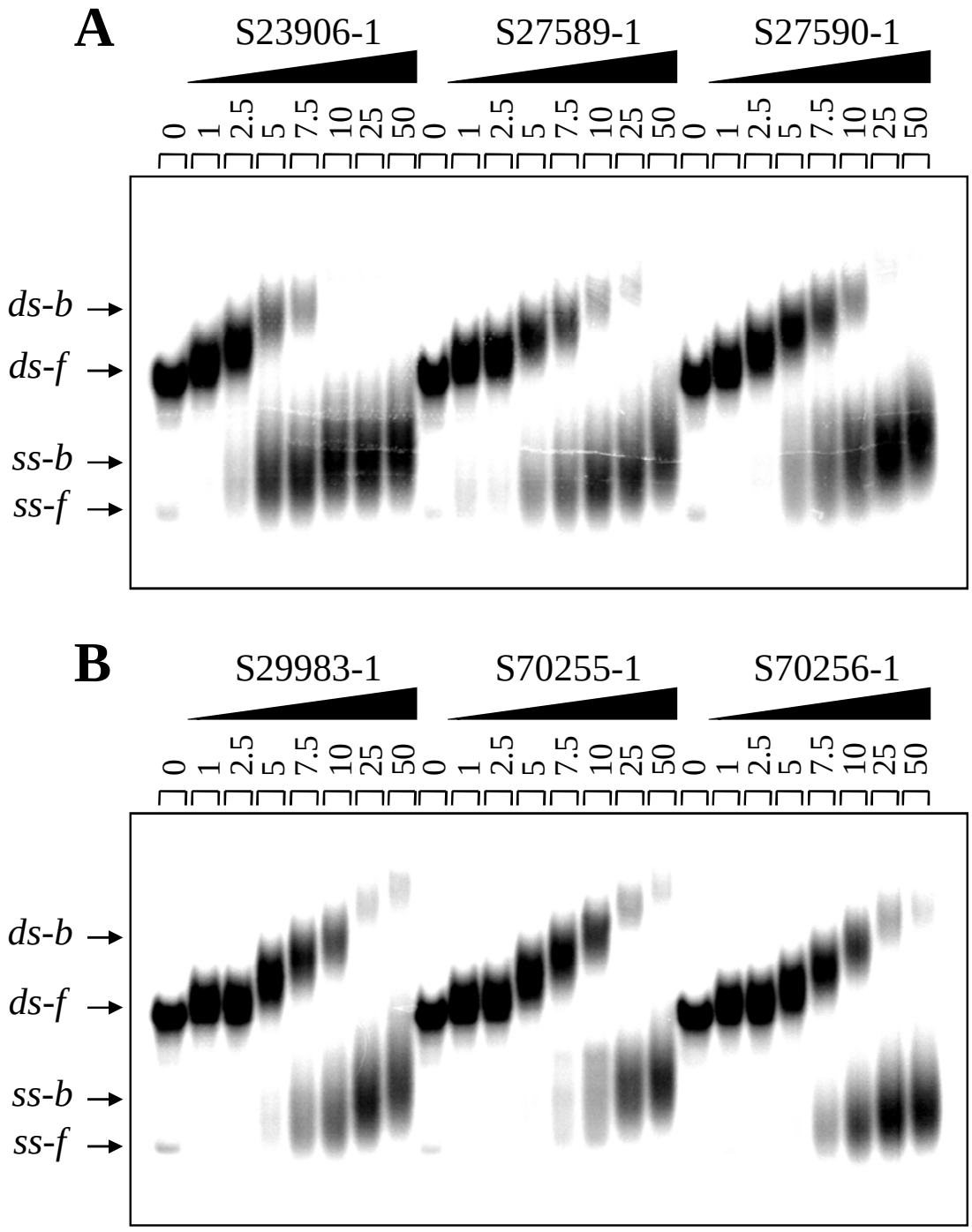

Molecular Pharmacology Fast Forward. Published on September 14, 2009 as DOI: 10.1124/mol.109.057554
This article has not been copyedited and formatted. The final version may differ from this version.

Figure 9